WILEY | Hindawi

Research Article

Prediction Model for Long-Term Bridge Bearing Displacement Using Artificial Neural Network and Bayesian Optimization

Ali Turab Asad,[1] Byunghyun Kim,[2] Soojin Cho,[2] and Sung-Han Sim [3,4]

[1]*Department of Civil, Architectural and Environmental System Engineering, Sungkyunkwan University, Suwon 16419, Republic of Korea*

[2]*Department of Civil Engineering, University of Seoul, Seoul 02504, Republic of Korea*

[3]*School of Civil, Architectural Engineering and Landscape Architecture, Sungkyunkwan University, Suwon 16419, Republic of Korea*

[4]*Department of Global Smart City, Sungkyunkwan University, Suwon 16419, Republic of Korea*

Correspondence should be addressed to Sung-Han Sim; ssim@skku.edu

Bridge bearings are critical components in bridge structures because they ensure the normal functioning of bridges by accommodating the long-term horizontal movements caused by changing environmental conditions. However, abnormal structural behaviors in long-term horizontal displacement are observed when the structural integrity of bridge structures is degraded. This study aims to construct an accurate prediction model for long-term horizontal displacement under varying external environmental conditions to support the reliable assessment of bridge structures which has not been fully explored in previous studies. The main challenge in developing an accurate prediction model lies in modeling the influencing factors that accurately simulate the effect of external environmental conditions on long-term horizontal displacement. To enhance the prediction accuracy in the proposed study, the surrounding environmental effects by considering the relationship between the current and past displacements in addition to air temperature, thermal inertia, and solar radiation are modeled as critical influencing factors. In addition, a data-driven method based on an artificial neural network (ANN) integrated with Bayesian optimization (BO) is employed to model and predict long-term horizontal displacement with the adopted critical influencing factors. An overpass bridge equipped with bearing displacement monitoring and temperature sensors is used to validate the robustness and effectiveness of the proposed method. The analysis of the results concludes that the proposed method can generate an accurate and robust long-term horizontal displacement prediction model that supports a reliable anomaly detection approach for early warning systems of bridge structures.

1. Introduction

Bearings are considered a key component for maintaining the normal operation of bridge structures because they help transmit loads from the superstructure to the substructure while accommodating horizontal movements [1]. Bridge structures exhibit abnormal structural behavior when their serviceability and structural integrity are compromised. The horizontal displacement of bridge bearings, which reflects the overall bridge behavior, is a prominent indicator for assessing the structural condition of bridge structures [2, 3]. Therefore, changes in the horizontal displacement of bridge bearings, regarded as anomalous behavior, are a crucial issue that raises concerns regarding bridge maintenance and structural safety.

Structural health monitoring (SHM) is an effective approach to the maintenance and safety evaluation of bridge structures [4]. SHM systems for bridges measure data related to the structural response and surrounding environmental variations to evaluate their structural performance [5–7]. Prior studies in the SHM field that focused on bridge monitoring highlighted the significance of temperature effects on the long-term structural behavior of bridge components [3, 8–11], along with an emphasis on systematic

approaches to account for temperature effects in the data interpretation technique to ensure effective assessments of their structural condition. Thus, temperature-based data interpretation (TBDI) techniques in SHM have received significant attention in recent years for evaluating the structural condition of critical bridge components [2, 12–15]. As the horizontal displacement of bridge bearings is mostly governed by diurnal and annual temperature variations [3, 11], the characterization of long-term horizontal displacement in response to temperature fluctuations can yield substantial information for assessing their structural performance using the TBDI approach.

The TBDI technique in SHM detects damage and provides a warning about anomalous structural behavior by analyzing and separating temperature-induced responses from long-term measurements [15]. Two different methods can be used to deal with the temperature effects for anomaly detection using the TBDI technique. The first method relies only on the structural response (i.e., the output-only method) and treats the temperature effect as undesirable noise or an embedded variable that is discarded from the measured response using numerical techniques for anomaly detection [16, 17]. However, this method offers limited success as the TBDI technique for SHM. The effect of daily and annual temperature variations on the measured response is substantial compared with that of other external and environmental loads [11, 13, 18]. Therefore, there it is necessary to consider the temperature-induced response rather than ignoring it to effectively detect the anomalous structural behavior using the TBDI approach [14, 15]. The second method explicitly accounts for the temperature effect on the measured response by modeling the relationship between the temperature variation and temperature-induced response (i.e., the input-output method) and thus offers more promise. The residuals obtained as a discrepancy between the measured and predicted temperature-induced responses (TIR) can be analyzed for anomaly detection [19–21]. Accordingly, the effectiveness of the TBDI technique for detecting anomalous structural behavior and its gradual trend, analyzed based on the time histories of the residuals, seems to depend on the reliability of the predicted horizontal response based on temperature fluctuations. Thus, it is necessary to develop an appropriate TBDI approach that can predict the temperature-induced bearing response to ensure bridge maintenance and structural safety.

Existing TBDI approaches for SHM can be broadly divided into two categories: model-based and data-driven approaches. Model-based approaches are based on numerical finite element (FE) models to identify intrinsic changes in measured TIR [3, 22, 23]. The initial FE models should undergo a calibration process to obtain a better prediction of TIR, which is currently undergoing exhaustive research [3, 24, 25]. However, the application of FE models to TBDI from long-term SHM remains limited because incorporating FE models with varying environmental conditions (most importantly temperature) having a significant influence on the long-term structural behavior is challenging, and thus, the prediction accuracy can be undermined [15, 20, 26]. In addition, it is difficult to assess the accuracy of the computed FE models because of modeling uncertainties and assumptions (e.g., boundary conditions, chosen model behavior and geometry, and simplified structural elements) [27, 28]. Data-driven approaches offer promise for addressing the shortcomings of model-based approaches by adopting measured responses instead of FE models to understand structural behavior. Data-driven approaches for TBDI utilize available long-term measurements to establish baseline conditions for normal structural behavior. Subsequently, new measurements are analyzed against the measurements predicted by data-driven methods to detect deviations from the normal baseline condition [20]. Therefore, data-driven methods are robust and offer great promise for long-term SHM, which can be utilized to detect and identify changes in structural behavior using the TBDI technique.

Data-driven methods can efficiently learn the complicated input-output relationships of the system using long-term measurements without requiring extensive prior structural knowledge. Therefore, relevant studies have focused on predicting the TIR of bridge structures by explicitly modeling the relationship with temperature variations in bridges using data-driven methods [12, 21, 29–35]. The prediction of TIR using the established temperature-displacement relationship (data-driven) model can then be utilized to assess the bridge's structural condition. However, bridge structures can have complex nonlinear temperature distributions [15], and therefore, not all temperature measurements are strongly correlated to the thermal response at a specific location [33, 36]. Consequently, the prediction accuracy of data-driven TBDI is inevitably influenced by the location of the temperature sensors installed on the bridge structure [30, 33]. Air temperature affects bridge structures globally and is considered a major factor that causes bridge temperature variations [37], thus showing a strong correlation with the TIR. Therefore, air temperature is utilized as an influencing factor in data-driven TBDI to efficiently predict the TIR such as strain, girder deflection, and horizontal displacement [38–40]. However, previous studies [38–40] could not model the thermal inertial and seasonal solar radiation variation effects, and this can affect the prediction accuracy of the TIR, which in turn affects the reliability of the TBDI approach. The difference between the bridge and air temperature exists [41] because changes in air temperature are not immediately reflected in the bridge temperature, owing to the thermal inertial effect, and follows the seasonal variation attributed to the direct solar radiation and local heat island (irradiation from the ground) effect [38, 42]. The strong and intense solar radiation and the irradiation from the ground during the summer season increase the bridge temperature significantly above the air temperature compared to the relatively weak sunlight and cold ground in the other seasons [38]. Thus, seasonal solar radiation variation affects the bridge temperature in addition to air temperature, which significantly influences the TIR and should be considered to enhance the prediction accuracy of data-driven methods for reliable TBDI. Furthermore, the bridge temperature in addition to air temperature and seasonal solar radiation is influenced by

other surrounding environmental factors and the residuals attributed to such external environmental effects in data-driven methods should be considered for an accurate and reliable TBDI.

Considering the limitations in previous studies to comprehensively model the external environmental effects for thermal response modeling, this research focuses on developing an accurate data-driven method that solves a regression problem by employing critical influencing factors to efficiently model and predict the long-term horizontal displacement of bridge bearings. The critical influencing factors for effectively modeling the bearing horizontal displacement were selected based on the potential sources of heat exchange between the bridge structures and the external surrounding environment. The relationship between the critical influencing factors and bearing horizontal displacement may not be always linear in practice but rather can be complex and nonlinear depending upon the bridge's structural characteristic and bearing type. Therefore, an artificial neural network (ANN) is employed as a data-driven model because of its ability to efficiently model the linear and nonlinear relationships between the influencing factors and structural response compared to traditional statistical regression models while dealing with high-dimensional data-mapping problems [43–47]. Several related research studies owing to the capability of ANN to effectively model and predict the bridge responses are reported in [30, 39, 48–52]. However, the ANN model requires tuning of hyperparameters, which is critical for increasing modeling flexibility and enhancing prediction performance [47, 48, 50, 53]. It is challenging to determine the optimum ranges of the hyperparameters quickly and robustly via conventional trial-and-error methods because many hyperparameters of the ANN model have coupling effects with a vast search space owing to their wide range of numerical values [54, 55]. To overcome this issue, Bayesian optimization (BO), which emerged as a powerful tool for hyperparameter optimization [56–59], was integrated with the ANN model to solely search for the optimal ANN hyperparameters in the proposed study. Long-term bearing horizontal displacement and air temperature data collected from a sensor network installed on a bridge with a total span length of 6345 m were utilized to explore and validate the effectiveness of the proposed method.

2. Background

2.1. Artificial Neural Network.
The ANN, introduced by McCulloch and Pitts [60], is a data-driven model that is extensively used in the fields of machine learning and data mining. The ANN model was developed based on the functioning of the biological nervous system of the human brain. The learning process is the main idea of the ANN model, and the model involves a network of interconnected neurons that work together to discover complex relationships in the data to be analyzed. Research studies have been conducted in the field of SHM to predict the structural response of bridge structures owing to the capability of the ANN model to effectively learn and simulate the behavior of

complex structural systems [30, 39, 48–52]. During ANN modeling, no hypotheses or preconstraints are necessary, which allows the ANN model to have a significant advantage over traditional computational models [47]. Furthermore, the ANN model is robust against outliers [46] and is a powerful tool for high-dimensional data-mapping regression problems, exploiting the advantages of parallel processing [43, 48, 50]. ANN was employed as a data-driven model to predict the horizontal displacement in this study owing to its capability to accurately model the linear and nonlinear relationships between the influencing factors and structural response compared to traditional statistical regression models.

Figure 1 shows that the feedforward multilayer perceptron (MLP) structure comprises three layers connected by artificial neurons and is considered a shallow ANN model that is widely used in many applications. An input layer receives the influencing factors for a specific problem and propagates them to hidden layers. The hidden layers use an activation function to process the weighted sum of incoming signals and output them to the next layer, which can be either another hidden layer or output layer [48]. For the sake of simplicity, the following is a description of a single hidden layer MLP:

$$H_l = f_0 \left(W_0 \times X_k \right) + b_0, \tag{1}$$

$$\widehat{Y} = f_1 \left(W_1 \times H_l \right) + b_1, \tag{2}$$

where X_k are the number of influencing factors at the input layer, H_l are the outputs of hidden layer, $\widehat{Y}$ is the predicted response variable, f_0, W_0, and b_0 are the activation function, weight matrix, and bias vector of the hidden layer, respectively, while f_1, W_1, and b_1 are the activation function, weight matrix, and bias vector of the output layer, respectively. The ANN model is trained to compute weight matrices and bias vectors using the gradient descent method. During the training phase, the ANN model iteratively reduces the mean square error (MSE) of the dataset by modifying the collection of known input-output pairings until the output value falls below a certain threshold.

2.2. Bayesian Optimization for ANN Hyperparameter Tuning.
The effectiveness and prediction accuracy of the ANN model depend on its architecture and training parameters, regarded as ANN hyperparameters, which should be selected carefully to enhance the ANN performance [46–48, 50, 53–55]. However, there is no consensus regarding the appropriate method for selecting the ANN hyperparameters. Trial-and-error-based optimization is commonly adopted to fine-tune the hyperparameters of the ANN model. In this approach, different ANN models are generated by varying the parameters and evaluating the prediction performance of each model. The ANN model with the best prediction accuracy is then selected for further assessment [46–48]. However, the trial-and-error method is computationally expensive and labor-intensive because many ANN hyperparameters have coupling effects with a vast search space, which makes it difficult to quickly determine their optimal ranges, thus necessitating the use of robust optimization approaches.
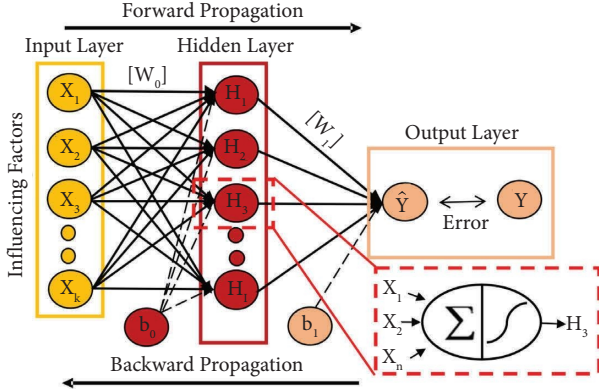
FIGURE 1: Feedforward multilayer perceptron structure with a single hidden layer.

BO internally retains a Gaussian process (GP) model (i.e., probabilistic surrogate model) of the objective function, which makes it particularly ideal for the global optimization of black-box objective functions that are difficult to evaluate. In BO, the loss is modeled as an objective function $f(\theta)$ of the hyperparameters θ, and it searches for its global minimum value drawn from the GP prior which can be expressed as

$$\theta^* = \arg\min f(\theta), \theta \in A, \tag{3}$$

$$f(\theta) \sim \text{GP}\left(\mu(\theta), k\left(\theta, \theta'\right)\right), \tag{4}$$

where A represents the search space of θ, and $\mu(\theta)$ and $k(\theta, \theta')$ are the mean function and covariance function of the GP respectively. The $\mu(\theta)$ captures the expected value of the objective function $f(\theta)$ at a given hyperparameter setting, and the $k(\theta, \theta')$ captures the similarity or correlation between the objective function $f(\theta)$ values at different hyperparameter settings. The BO explores the posterior distribution of the objective function $f(\theta)$ using the prior distribution of the objective function $f(\theta)$ with the sample information as evidence. The posterior distribution at each new evaluation of the objective function $f(\theta)$ can be defined as follows:

$$f(\theta^+) \sim \text{GP}\left(\mu(\theta^+), \sigma^2(\theta^+)\right), \tag{5}$$

where $\mu(\theta^+)$ and $\sigma^2(\theta^+)$ are the posterior mean function and variance function, respectively. The posterior information is then utilized to identify where the objective function $f(\theta)$ is minimized, based on a criterion represented by the acquisition function $\alpha(\theta)$. The role of the acquisition function $\alpha(\theta)$ is to measure the expected improvement $\text{EI}(\theta)$ in the objective function $f(\theta)$ while discarding the values that would increase it. The expected improvement $\text{EI}(\theta)$ can be calculated as follows:

$$\text{EI}(\theta) = \left(\mu(\theta^+_{\text{best}}) - \mu(\theta^+)\right)\Theta(z) + \varphi(z), \tag{6}$$

where $\mu(\theta^+_{\text{best}})$ is the lowest observed value of the posterior mean function, Θ is the standard normal cumulative density function, φ is the standard normal probability density function, and $z = (\mu(\theta^+) - \mu(\theta))/(\sigma(\theta))$. The acquisition function is employed iteratively in an exploration (sampling from the areas of high uncertainty) and exploitation (sampling from that with high values) manner to determine the next hyperparameter configuration by maximizing the acquisition function over the GP. More detailed information on BO can be found in [56, 57]. The BO method can determine the optimal parameter configuration with relatively fewer iterations and is often significantly faster than the trial-and-error method [57–59]. Accordingly, in the present study, the ANN was integrated with BO, as illustrated in Table 1, to solely search for optimal ANN hyperparameters that generate a robust and accurate data-driven prediction model for long-term horizontal displacement.

3. Bearing Horizontal Response Prediction Methodology

This section describes the proposed modeling and prediction method for the horizontal displacement of bridge bearings, with a comprehensive consideration of the external surrounding environment. Previous studies have not comprehensively explored the use of environmental factors in combination as input information to data-driven models for thermal response modeling. To predict the long-term bearing responses accurately, the proposed prediction model employs critical influencing factors to effectively model the external environmental effects on the horizontal displacement to support a reliable early warning system.

3.1. Horizontal Displacement Modeling of Bridge Bearings. This study aimed to construct a prediction model for the horizontal displacement of bridge bearings. However, the main challenge lies in the selection of influencing factors to accurately model horizontal displacement under changing external environmental conditions. In addition to air temperature and solar radiation as the major influencing factors, other surrounding environmental factors (e.g., wind) [15] can influence the horizontal displacement, as shown in Figure 2. The prediction accuracy can be improved by appropriately selecting the influencing factors for the horizontal displacement modeling. Therefore, considering the potential sources of heat exchange between the bridge structure and the external surrounding environment, the influencing factors listed in Table 2 were adopted in the proposed study to model the horizontal displacement and were examined based on the prediction accuracy.

To demonstrate the feasibility of the proposed method, an ANN was employed to model the relationship between the bearing horizontal displacement and the adopted influencing factors that reflect the external environmental effects, as listed in Table 2. Variable set S_1 considers only the air temperature T_0 as an effective factor for modeling the horizontal displacement, where T_0 represents the air temperature at the current displacement measurement time. The segmented air temperature T_{p-q} along with T_0 as proposed in [61–63] was adopted in the variable set S_2 to model the air temperature effect on the horizontal displacement while

TABLE 1: ANN integration with Bayesian optimization for hyperparameter tuning.

| |
|---|
| Objective function $f(\theta)$ to be optimized: $\theta^* = \text{argmin } f(\theta), \theta \in A$ where A = search space of ANN hyperparameters and $\theta = \{\theta_1, \theta_2, ..., \theta_n\}$ = vector of ANN hyperparameters from defined search space. |
| **Algorithm: ANN with BO** |
| 1: **For** $j = 1,2,3,...$ |
| 2: Find θ_j by maximizing the acquisition function $\alpha(\theta)$ over the GP: $\theta_j = \text{argmax} \alpha(\theta \mid D_{1: j-1})$ |
| 3: Calculate the prediction error $E(\theta_j)$ through ANN with θ_j determined in step 2 |
| 4: Augment the data $D_{1:j} = \left\{ D_{1:j-1}, (\theta_j, E(\theta_j)) \right\}$ and update the posterior distribution of GP |
| 5: **End for** |
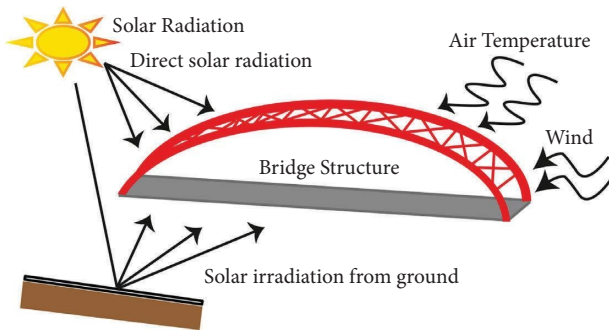
FIGURE 2: Influencing factors adopted for bearing horizontal displacement modeling.

TABLE 2: Dataset configuration for bearing horizontal displacement modeling.

Input variable sets based on adopted environmental influencing factors
$S_1 = \{T_0\}$
$S_2 = \{T_0, T_{1\text{-}2}, T_{3\text{-}4}, T_{5\text{-}6}, d\}$
$S_3 = \{T_0, T_{1\text{-}2}, T_{3\text{-}4}, T_{5\text{-}6}, D_1, d\}$
$S_4 = \{T_0, T_{1\text{-}2}, T_{3\text{-}4}, T_{5\text{-}6}, D_2, d\}$
$S_5 = \{T_0, T_{1\text{-}2}, T_{3\text{-}4}, T_{5\text{-}6}, D_3, d\}$
$S_6 = \{T_0, T_{1\text{-}2}, T_{3\text{-}4}, T_{5\text{-}6}, D_4, d\}$
$S_7 = \{T_0, T_{1\text{-}2}, T_{3\text{-}4}, T_{5\text{-}6}, D_5, d\}$
$S_8 = \{T_0, T_{1\text{-}2}, T_{3\text{-}4}, T_{5\text{-}6}, D_6, d\}$

considering the thermal inertia (lag between the displacement response and air temperature) effect. Variable $T_{p\text{-}q}$ represents the average air temperature from p to q observations before the current horizontal displacement measurement. According to previous studies [61–63], the segmented air temperature $T_{p\text{-}q}$ effectively reflects the influence of the air temperature with a lag effect on the displacement variation. Therefore, the segmented air temperature $T_{p\text{-}q}$ variables were adopted as the influencing factors for horizontal displacement modeling. In addition, in variable set S_2, the thermal effect attributed to the seasonal variation in solar radiation on the horizontal displacement was modeled with variable d, which represents the day of the year from the beginning of the measurement. Variable d simultaneously captures the time and season of the year

[46]. Furthermore, the surrounding environmental factors affecting the horizontal displacement, in addition to air temperature and seasonal solar radiation, which are complex to model explicitly, were reflected by the lagged displacement variable D_n in the variable sets S_3–S_8. The lagged displacement variable D_n captures the relationship between current and n previous displacement observations. The maximum lagged observations for the $T_{p\text{-}q}$ and D_n variables considered in the present study that can have a significant influence on the current displacement measurement is six than going beyond further in time.

3.2. ANN Model Integrated with Bayesian Optimization.

BO is utilized in the proposed study to solely determine the optimal ANN hyperparameters, and a hybrid model is introduced to enhance the prediction accuracy. The search space for the ANN hyperparameters selected in this study is presented in Table 3.

(1) The number of hidden layers determines the computational speed and learning efficiency of the ANN model. According to previous studies [30, 46–48], a single hidden layer can solve any complex function approximation problem. Thus, the number of hidden layers was fixed as one in the proposed study, which considers the computational cost.

(2) The number of hidden neurons in a hidden layer during ANN modeling is generally selected between the number of input and output variables to avoid overfitting or underfitting problems owing to unnecessarily many or insufficient hidden neurons, respectively [64]. Considering this along with the computational cost, the search range for hidden neurons was set accordingly in the interval $[1, 2^{n+1}]$, where n represents the maximum number of input variables in the proposed study [54, 55].

(3) Commonly used activation functions and backpropagation training algorithms that provide acceptable accuracy for function approximation problems [30, 47, 48, 50, 65] are selected to construct the search space for BO. The activation function search space includes linear, tangent-sigmoid, and log-sigmoid activation functions, whereas the backpropagation training algorithm search space includes gradient descent, Levenberg-Marquardt, and Bayesian regularization. The linear transfer function was fixed for the output layer [55].

(4) Training parameters such as learning rate (lr), momentum constant (mc), and Marquardt parameter (μ) used in their respective backpropagation algorithms can have any value between 0 and 1 depending on the complexity of the data, and therefore, the typical ranges for training parameters were selected accordingly [53, 64].

The ANN prediction performance, as aforementioned, depends on the optimal parameters to train the ANN model determined within the defined search space using BO in the

TABLE 3: Hyperparameter search space for the Bayesian optimization.

Hyperparameters	Hyperparameters search space
Number of hidden neurons	[1, 128]
Activation function	{linear, tangent-sigmoid, log-sigmoid}
Training algorithm	{gradient descent, Levenberg-Marquardt, Bayesian regularization}
Learning rate (lr)	[0.001, 1]
Momentum constant (mc)	[0.8, 0.98]
Marquardt parameter (μ)	[0.0001, 0.1]

present study. For this purpose, the dataset used to train the ANN model was subdivided into training and validation datasets. To avoid overfitting (i.e., to obtain better fitting and generalization capability), the ANN model was trained with an early stopping technique [43], and its performance was based on the weighted root mean square error (RMSE) defined in equation (7) over the training and validation datasets was used as the objective function $f(\theta)$ for BO. In the weighted RMSE as the objective function to minimize, the weights assigned to the training and validation errors were 0.4 and 0.6, respectively. The reason can be justified as the validation dataset is kept unseen while training the ANN model to assess the generalization performance of the ANN model, more weightage value can be assigned to validation error as compared to training error in the $f(\theta)$ to be minimized to avoid overfitting. To evaluate the prediction capability of the optimized ANN model, the training and validation datasets were again combined into one dataset to retrain the ANN model with the obtained optimal parameters.

$$f(\theta) = w_1 \times RMSE_{train} + w_2 \times RMSE_{valid}, \quad (7)$$

where $RMSE_{train}$ and $RMSE_{valid}$ represent the root mean square error for the training and validation datasets, respectively; w_1 and w_2 represents the weights of training and validation errors, respectively, such that $w_1 + w_2 = 1$.

3.3. Model Assessment Metrics.

Once the optimally trained ANN model was generated through BO, its prediction performance was assessed to determine the effective environmental factors adopted for accurate horizontal displacement modeling. Four statistical assessment metrics commonly used for function approximation problems were employed in this study: RMSE, mean absolute error (MAE), Akaike information criterion (AIC), and coefficient of determination (R^2).

$$RMSE = \sqrt{\frac{1}{n} \sum_{i=1}^{n} (y_i - \widehat{y}_i)^2}, \quad (8)$$

$$MAE = \frac{1}{n} \sum_{i=1}^{n} |y_i - \widehat{y}_i|, \quad (9)$$

$$AIC = \sqrt{\frac{1}{n} \sum_{i=1}^{n} (y_i - \widehat{y}_i)^2 \, e^{(2k/n)}}, \quad (10)$$

$$R^2 = 1 - \frac{\sum_{i=1}^{n} (y_i - \widehat{y}_i)^2}{\sum_{i=1}^{n} (y_i - \overline{y}_i)^2}, \quad (11)$$

where n represents the number of observations, k represents the number of influencing factors, and y_i, $\widehat{y}_i$, and $\overline{y}_i$ represent the measured, predicted, and mean bearing displacement values, respectively. Regarding the assessment metrics, the RMSE and MAE represent the overall error distribution as model precision and accuracy, respectively; AIC corresponds to the robustness of the model considering the number of influencing factors while penalizing the most complex model; and R^2 indicates the goodness of fit.

3.4. Procedure for the Bearing Horizontal Response Prediction.

The procedure for the bearing horizontal displacement prediction with the optimized ANN model is illustrated in Figure 3 and can be described as follows.

3.4.1. Dataset Pre-processing.

The long-term air temperature and bearing horizontal displacement measurements collected from the safety monitoring system underwent the dataset pre-processing to make the ANN more efficient and to improve its estimation performance, which involves the following steps:

(i) The long-term monitored datasets were checked for constant, corrupt (unknown), and incorrect (outliers) values, and they were removed from the monitored datasets

(ii) After checking for suspicious and improper data, the influencing factors rearranged as input variable sets according to the dataset configuration, as described in Section 3.1, were modeled for horizontal displacement

(iii) The selected input variable set and target bearing response were then divided into training, validation, and testing datasets

(iv) Finally, the dataset normalization technique was employed to map the training, validation, and testing datasets to a uniform scale [+1, −1] and to eliminate the dimensional effects of the selected input variables on horizontal displacement modeling

3.4.2. Model Generation.

The ANN model was integrated with the BO algorithm (as illustrated in Table 1) in the model generation phase to determine its optimal hyperparameters within the defined search space based on the weighted RMSE as an objective function, as described in Section 3.2.
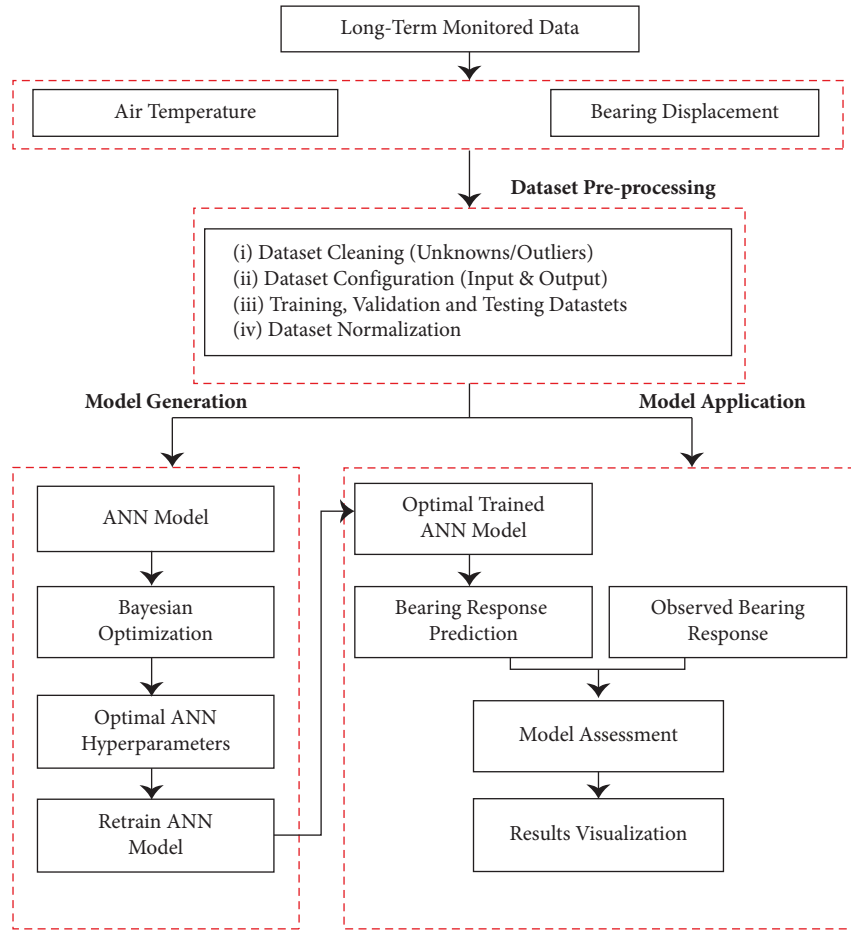
Figure 3: Bearing horizontal response prediction methodology flowchart.

3.4.3. Model Application. The optimally trained ANN model obtained using BO was used in the model application phase to predict the bearing horizontal displacement. The predictions of the ANN model were compared with the monitored horizontal displacement to evaluate its performance based on the assessment metrics described in Section 3.3. Finally, the horizontal displacement prediction results were visualized.

4. Case Study

4.1. Test Bed Bridge. The proposed prediction methodology was applied to an overpass bridge in South Korea, as shown in Figure 4**.** The target bridge constructed in 1999 was a steel-concrete composite bridge with a total number of 72 spans and a total length of 6345 m. The deck-pier connection was built using pot bearings, which allow for translation in the horizontal direction owing to the thermal effects in the target bridge structure. However, the relative horizontal displacement required between the deck and piers can be affected by anomalous structural behavior. Thus, this study intended to build a horizontal displacement prediction model for the implementation of a robust early warning decision-making system for bridge structures.

4.2. Description of SHM System Installed on the Test Bed. Figure 5(a) shows the SHM system installed in the test bed in 2020 to ensure the serviceability and structural safety of the target bridge [66]. Figure 5(b) shows the layout of the sensor network installed on the test bed of the target bridge. A computer vision system was used to measure the horizontal displacement of pot bearings. A CCTV camera was mounted underneath the test bed girder using a magnetic base at a distance of approximately 50 cm from the main target on the bearing support, as shown in Figure 6. A CCTV camera travels horizontally with the main girder while the target remains stationary and measures the relative displacement between the girder and bearing support, which is identical to that of the bridge bearing. CCTV cameras with image sensors having progressive scans (RGB CMOS $1/2.7''$) with full HD resolution (i.e., 1920×1080) and a lens with a focal length of 4 mm were used when the horizontal field of view was 90.2°. The air temperature near the monitored bearings was recorded using a platinum resistance temperature detector with a PT1000 sensor, which can measure the temperature with excellent accuracy over a wide range from −30 to 60°C. The CCTV image sensors measuring the bearing horizontal displacement considered in the proposed study are referred to as B_1–B_4 (B: bearing), as depicted in Figure 5(b).

(a)   (b)

FIGURE 4: Test bed: overpass bridge.

4.3. Long-Term Measurement. The horizontal bearing displacement and air temperature were recorded with a sampling period of 1 h for approximately 18 months from September 1, 2020, to February 13, 2022, using the SHM system. There were disconnections in the monitored datasets at the beginning of the measurements, which can occur in the long-term monitoring of in-situ structures because of a variety of issues, such as sensor malfunction, electricity problems, and visual interruption by light reflection and backlight [66]. The bearings' horizontal displacement caused by the dynamic live load was filtered out by recording static measurements with a sampling period of 1 h. The reason can be justified as the effect of the traffic load on the bearings' horizontal displacement is significantly small when compared to air temperature [11].

Figure 7 shows the overall trends in the monitored long-term horizontal displacement of the selected bearings (B_1–B_4) on the respective piers. The average air temperature and bearing (B_1) horizontal displacement monitored on Pier #1 were normalized by the range of each measurement to examine the relationship between the long-term measurements more closely, and the normalized measurements are plotted in Figures 8(a)–8(b). The effects of diurnal (daily) and annual (seasonal) air temperature variations can be reflected in the horizontal displacement over time by showing similar variation patterns. This confirms that the air temperature variations considerably influence the bearing horizontal response, having a strong correlation between them. Figures 8(c)–8(d) show the effects of thermal inertia and seasonal solar radiation on the monitored horizontal displacement. The horizontal displacement shows a small magnitude variation during the winter season compared to the summer season, and it also lags behind the air temperature. As discussed, although the seasonal solar radiation being the critical influencing factor in addition to air temperature for bearing horizontal displacement, the seasonal solar radiation variation was not monitored using the SHM systems installed at the test bed and was explicitly modeled with variable *d* as day of the year information. Furthermore, the horizontal displacement variation caused by the surrounding environmental effects at the current measurement time can be reflected in the prior displacement information. Therefore, it is necessary to select the influencing factors that effectively model

external environmental effects for an accurate horizontal displacement prediction model.

5. Evaluation of Proposed Method and Discussion of the Results

The major contribution of this study is the modeling of external environmental effects with the adopted critical influencing factors for predicting the long-term horizontal displacement of bridge bearings. The average air temperature and horizontal displacement of bearings B_1–B_4 on the respective piers measured between September 1, 2020, and February 13, 2022, were utilized to evaluate the proposed methodology. Note that the displacement sensors of the selected bearings exhibited the least data loss. Incorrect (outliers) and missing data points from the beginning of the long-term measurements were removed from the monitored datasets to obtain a continuous and compatible measurement time history for a robust and efficient prediction model. The ANN model integrated with BO was trained with the adopted influencing factors rearranged as input variable sets for horizontal displacement modeling over a period from September 1, 2020, to October 31, 2021. The training period for determining the optimized ANN model via BO was subdivided into training and validation datasets. The one-year period from September 1, 2020, to August 31, 2021, containing sufficient information regarding the full range of variability was used as the training dataset, while the period from September 1, 2021, to October 31, 2021, was used as the validation dataset. To evaluate the prediction performance of the optimally trained ANN model for bearing horizontal displacement, the testing dataset corresponding to the period from November 1, 2021, to February 13, 2022, was utilized.

5.1. Optimal ANN Model. This section discusses the results from the model generation phase wherein the ANN model was integrated with BO to determine the optimal parameters that enhance the ANN performance. The implementation of the ANN model with BO was programmed using MATLAB on a PC (Intel Core i7-10700 processor and 16 GB RAM). The optimal parameters were determined within the defined search space, based on the weighted *RMSE* defined in equation (7) as an objective function for the BO. Figure 9
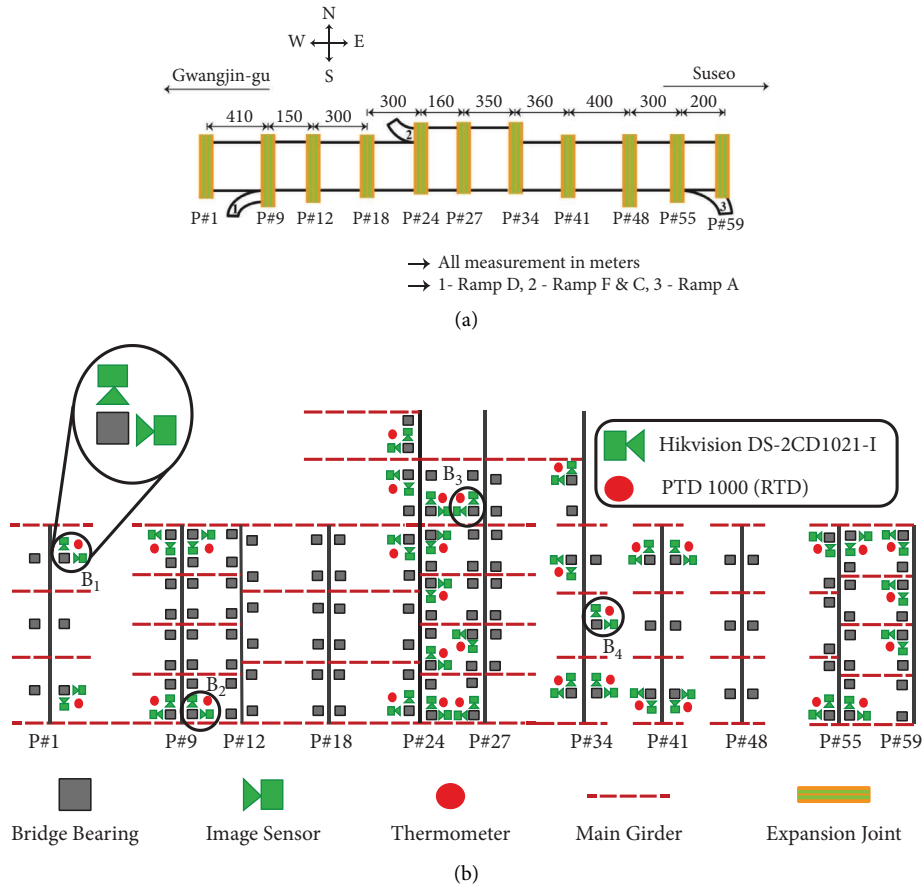
(a)

(b)

FIGURE 5: Sensor layout on the bridge [66]: (a) bridge layout and (b) sensor locations.

(a)

(b)

FIGURE 6: Displacement monitoring system: [66] (a) configuration of the measurement system and (b) target installed on bearing support.

shows the performance of the optimized ANN models for each adopted set of influencing factors. The input variable sets S_3–S_8 with the proposed influencing factors reflecting the external environmental effects on bearings (B_1–B_4) horizontal displacement resulted in a lower prediction error (*RMSE*) over the training and testing periods compared to influencing factors adopted in the S_1 and S_2 sets. However, the best prediction performance (least *RMSE* over the testing period as unseen data) with the optimally trained ANN model among the input variable sets S_3–S_8 is obtained with the critical influencing factors adopted in sets S_4 and S_5 for

bearings B_1–B_4 as shown in Figures 9(a)–9(d). Furthermore, Figure 10 shows the convergence of the weighted *RMSE* as an objective function $f(\theta)$ obtained using the optimal hyperparameters configuration after employing 30 iterations, as recommended by [59, 67]. Note that Figures 10(a)–10(d) illustrate the objective function $f(\theta)$ convergence for the critical influencing factors that resulted in the best prediction performance for bearings B_1–B_4, along with the influencing factors adopted in sets S_1 and S_2. No significant improvement in the objective function $f(\theta)$ was observed during the additional iterations. For conciseness, Table 4
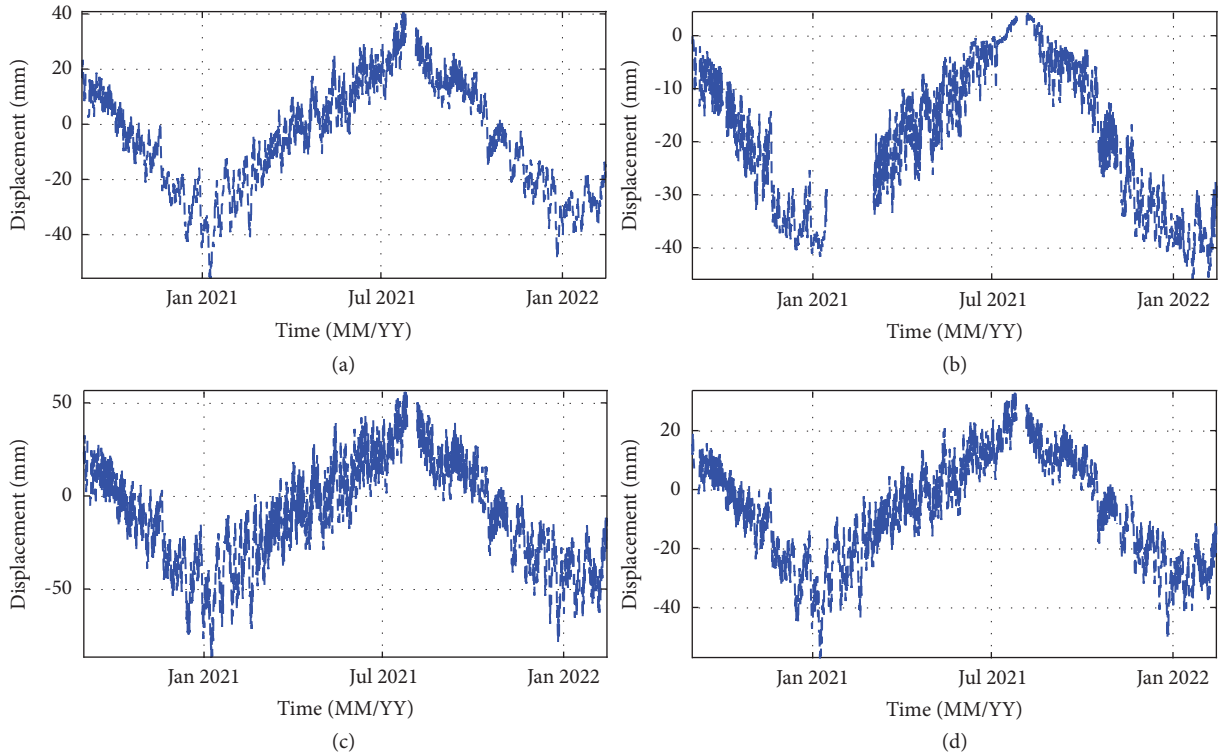
FIGURE 7: Measured long-term horizontal displacement: (a) B_1-Pier#1, (b) B_2-Pier#9, (c) B_3-Pier#27, and (d) B_4-Pier#34.
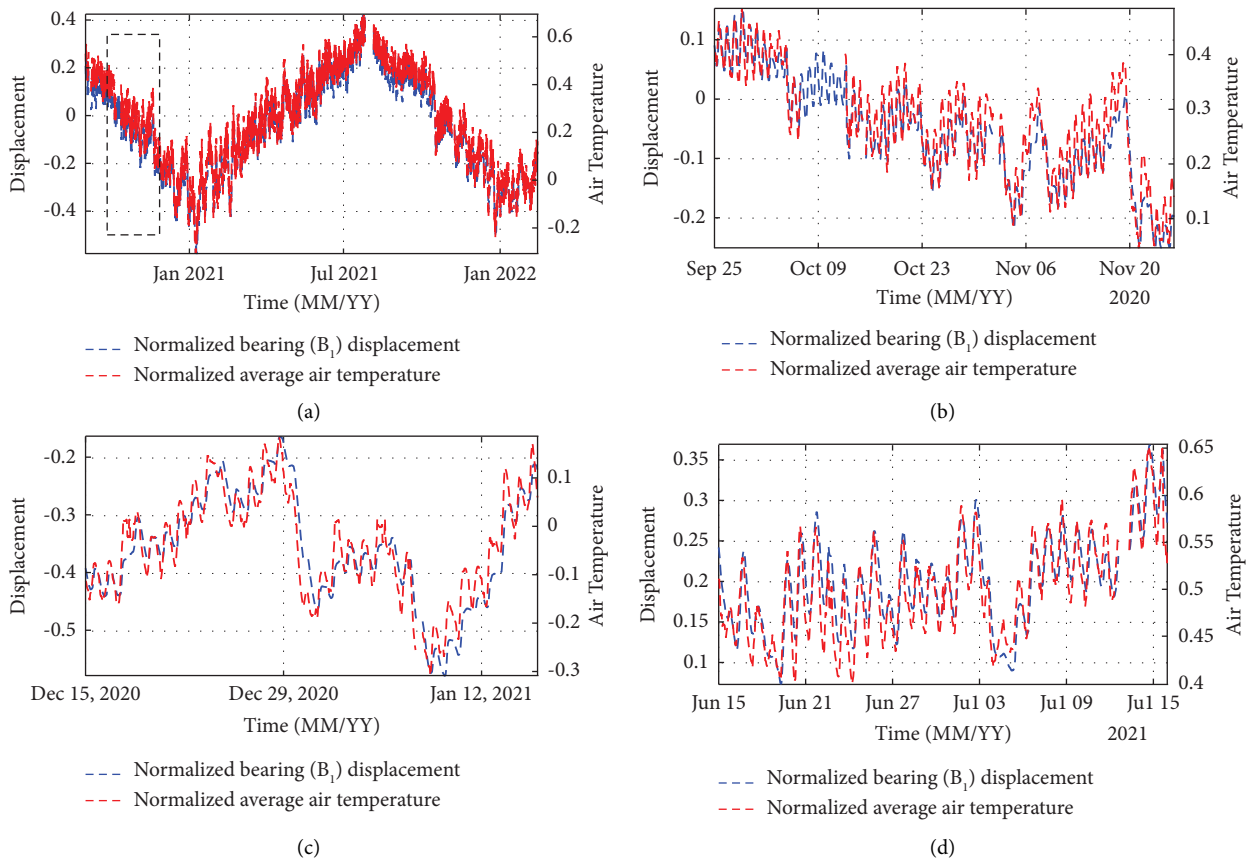

FIGURE 8: Normalized long-term measurements recorded by sensors on Pier#1: (a) normalized bearing (B_1) horizontal displacement and average air temperature, (b) zoomed view of the black dashed box, (c) zoomed view in the winter, and (d) zoomed view in the summer.
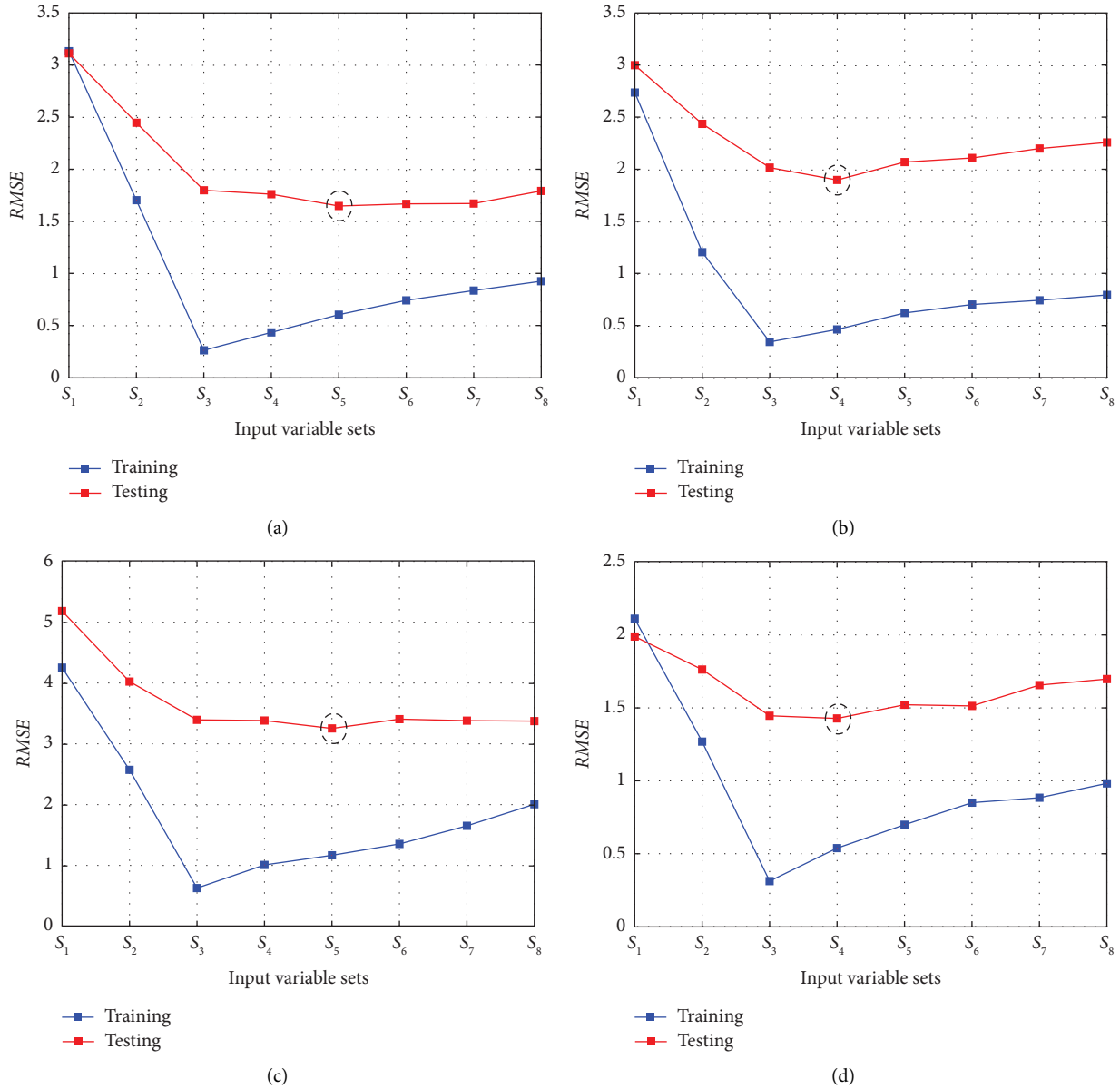
FIGURE 9: Performance of the optimized ANN models determined via BO for the adopted influencing factors: (a) B_1-Pier#1, (b) B_2-Pier#9, (c) B_3-Pier#27, and (d) B_4-Pier#34; the dotted circles indicate the best prediction accuracy.

summarizes the optimal parameters determined via BO only for the ANN model with critical influencing factors that resulted in the least prediction error for the horizontal displacement of the bridge bearings (B_1–B_4).

The BO was compared with the random search optimization approach in terms of prediction performance to further evaluate the effectiveness and robustness of BO for parameter tuning. The random search algorithm is commonly adopted to tune the hyperparameters of data-driven machine-learning models [58, 68]. For a fair comparison, a random search optimization technique was implemented on the same search space and datasets for the same number of iterations (i.e., 30) as those used for BO. Figures 11(a)–11(d) illustrate the performance of the optimized ANN model via BO and the random search algorithm, respectively, with critical influencing factors S_4 and S_5 for the horizontal displacement modeling of bearings B_1–B_4. As shown in Figures 11(a)–11(d), for the overall comparative computational cost (time in seconds), the ANN model optimized with BO exhibited significant superiority over the random search in terms of prediction accuracy for the testing dataset ($RMSE_{test}$) as our major concern. This can be
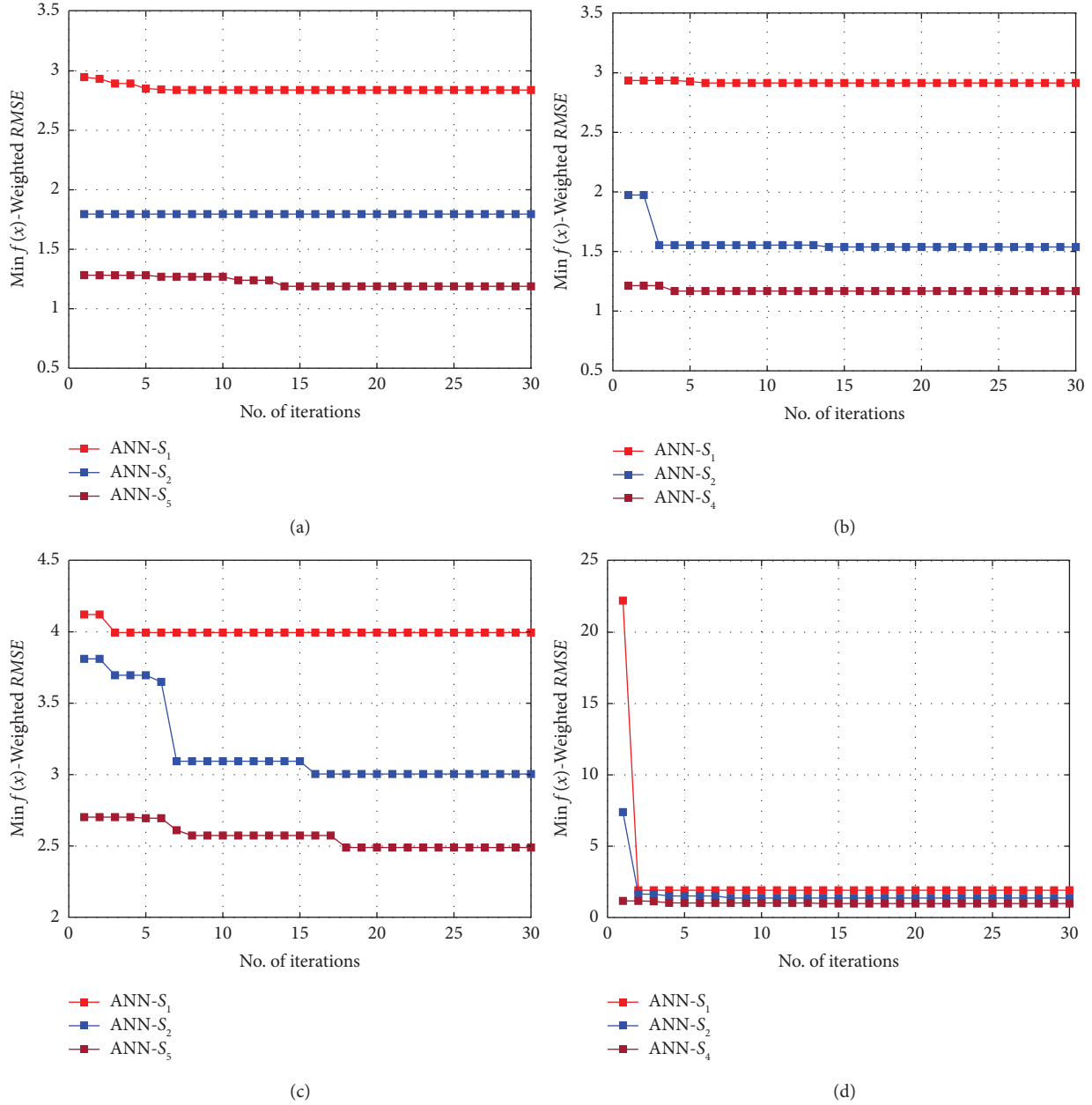
Figure 10: Convergence of the minimum objective function $f(\theta)$ through BO to obtain the optimal ANN parameters: (a) B_1-Pier#1, (b) B_2-Pier#9, (c) B_3-Pier#27, and (d) B_4-Pier#34.

Table 4: Optimal ANN hyperparameters obtained via Bayesian optimization.

Monitored bearings	Model-influencing factors	Hidden neurons	Activation function	Training algorithm	Training parameter
B_1-Pier#1	ANN-S_5	11	logsig	BR	$\mu = 0.0699$
B_2-Pier#9	ANN-S_4	110	logsig	BR	$\mu = 0.0611$
B_3-Pier#27	ANN-S_5	16	tansig	LM	$\mu = 0.0999$
B_4-Pier#34	ANN-S_4	10	tansig	LM	$\mu = 0.0008$

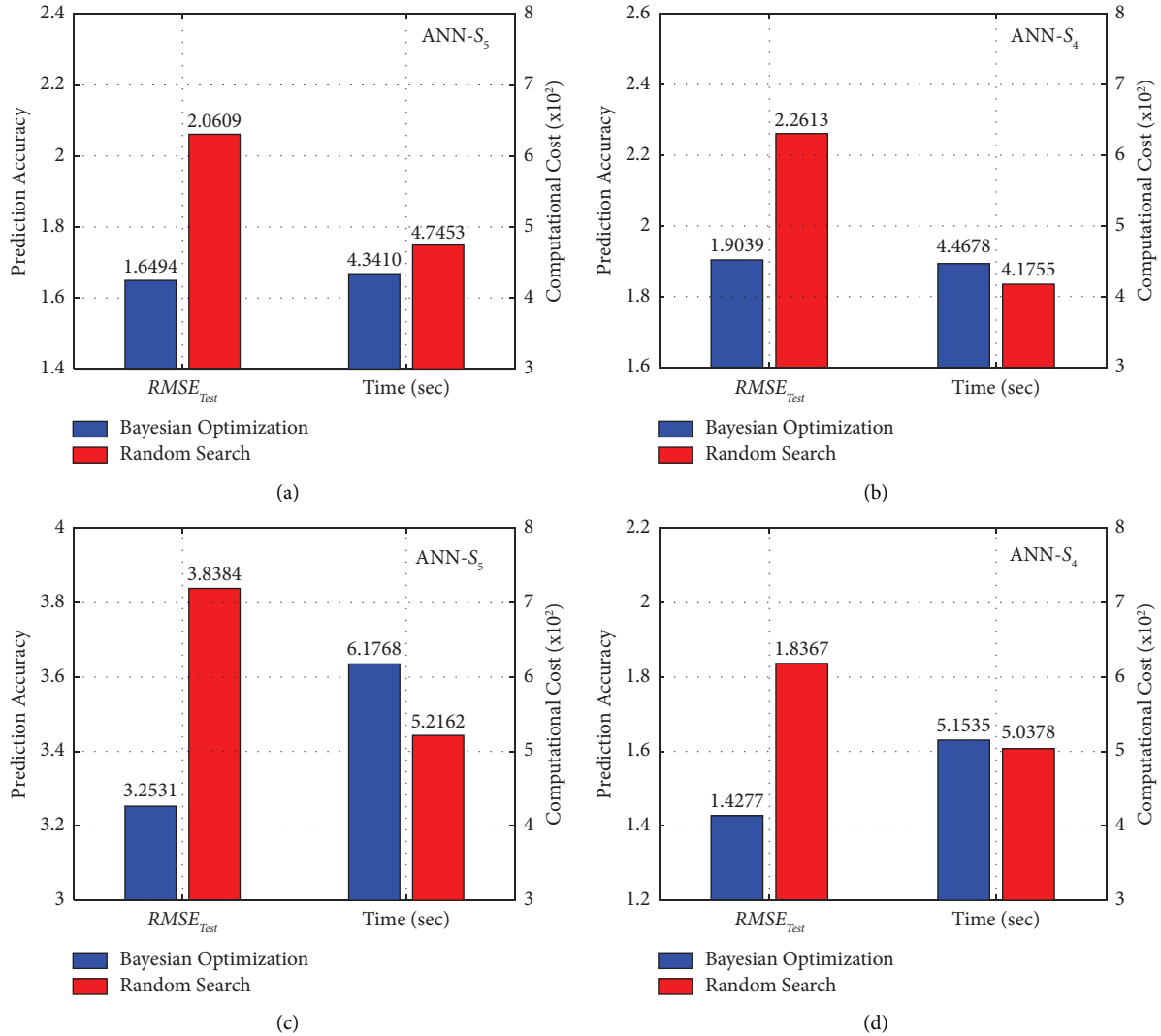logsig = log-sigmoid, tansig = tangent-sigmoid, BR = Bayesian regularization, LM = Levenberg–Marquardt.

FIGURE 11: Comparison of the optimized ANN models via optimization techniques with critical influencing factors: (a) B_1-Pier#1, (b) B_2-Pier#9, (c) B_3-Pier#27, and (d) B_4-Pier#34.

justified as the major drawback of the random search algorithm is that it ignores prior information regarding hyperparameter combinations in each iteration, which causes the risk of losing the optimal hyperparameters [58].

5.2. Model Assessment and Results Visualization. The results of the model application phase, in which the prediction performance of the optimized ANN model determined using BO was assessed and visualized, are presented in this section. The feasibility of the critical influencing factors S_4 and S_5 which effectively models the external environmental effects (as discussed in Section 5.1) on the horizontal displacement of bearings B_1-B_4 is compared with the influencing factors S_1 and S_2 in terms of assessment metrics. Note that S_1 simulates the air temperature effect only, whereas S_2 models the air temperature while considering the thermal inertia in addition to seasonal solar radiation effects on the horizontal displacement. Figure 12 presents the assessment

metrics of the testing dataset with the optimal ANN models for bearings B_1–B_4. As shown in Figures 12(a)–12(d), the optimized ANN model with the critical influencing factors S_4 and S_5 resulted in an accurate, precise, and robust model, which is indicated by the lower *RMSE, MAE,* and *AIC* values for ANN-S_4 and ANN-S_5 compared to ANN-S_1 and ANN-S_2. More specifically, the *RMSE* values for the ANN-S_4 and ANN-S_5 with respect to the variation ranges of the bearings, (B_1–B_4) horizontal displacement were very small and corresponded to 1.7037%, 4.4494%, 2.2740%, and 1.5772%, for the bearings B_1–B_4, respectively. This confirms the effectiveness of the ANN-S_4 and ANN-S_5 in predicting the bearings' (B_1–B_4) horizontal displacement without accumulating large prediction errors compared to ANN-S_1 and ANN-S_2. Additionally, ANN-S_4 and ANN-S_5 have a better goodness of fit for the horizontal displacement of the bearings (B_1–B_4), with R^2 values closer to 1 than ANN-S_1 and ANN-S_2.
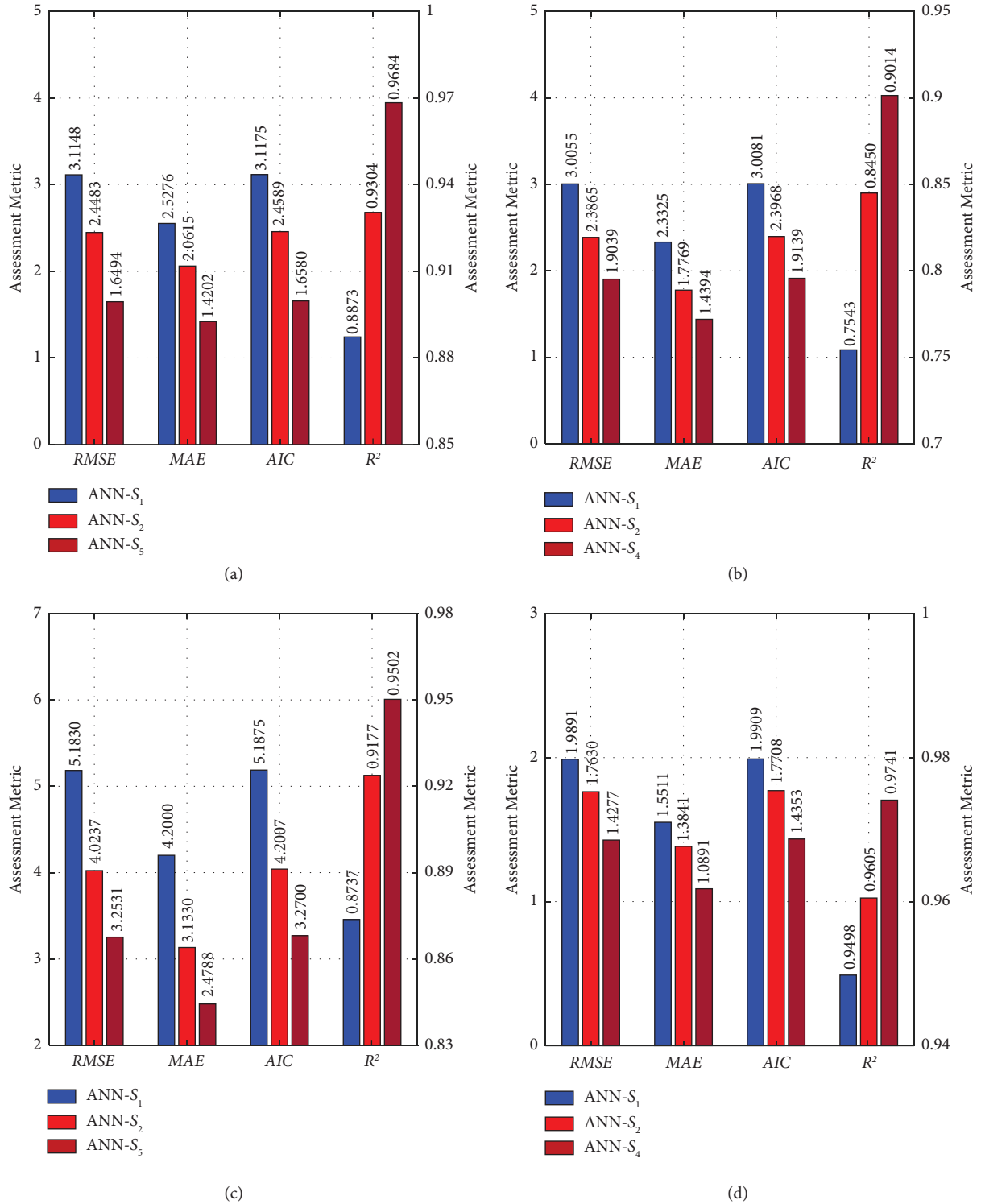
(a)

(b)

(c)

(d)

Figure 12: Performance comparison in terms of assessment metrics of the test dataset with the optimized ANN models: (a) B_1-Pier#1, (b) B_2-Pier#9, (c) B_3-Pier#27, and (d) B_4-Pier#34.

As an aspect of the result visualization, Figures 13-14 illustrate the prediction and amplitude of the prediction residual with critical influencing factors S_5 compared to S_1 for the horizontal displacement of bearings B_1 on Pier#1 and B_3 on Pier#27, respectively. Note that bearing B_3 has the largest prediction error among the considered bearings. The

optimized ANN-S_5 model, in contrast to the ANN-S_1 model, results in predictions that closely fit the measured horizontal displacement specifically at the daily extreme values and hence shows a small amplitude variation of the prediction error. Furthermore, when examining the overall prediction accuracy of the bearings' daily extreme (minimum and
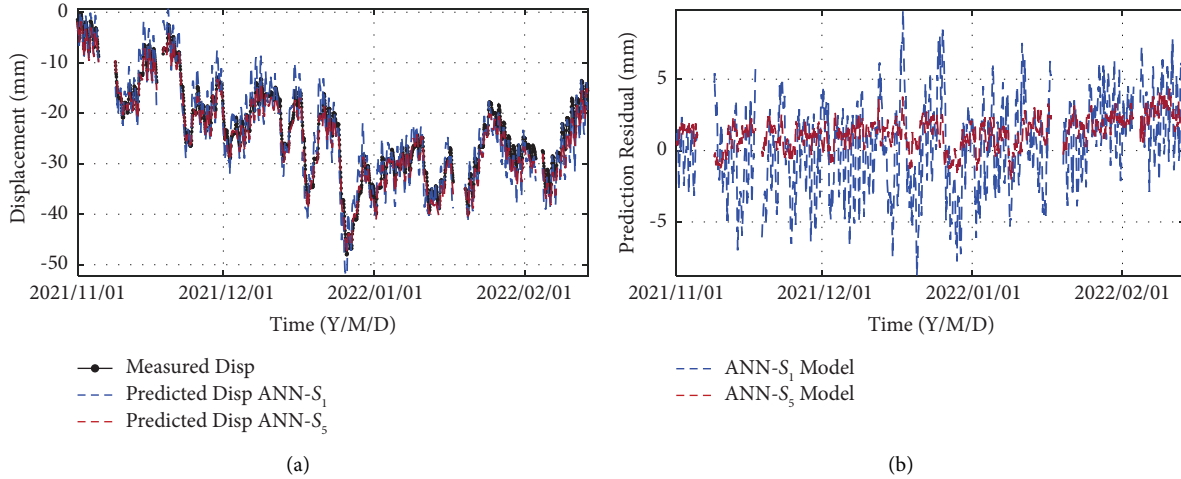
FIGURE 13: Results visualization of the optimized ANN-S_1 and ANN-S_5 models for B_1-Pier#1: (a) prediction results of the test dataset and (b) prediction residual of the test dataset.
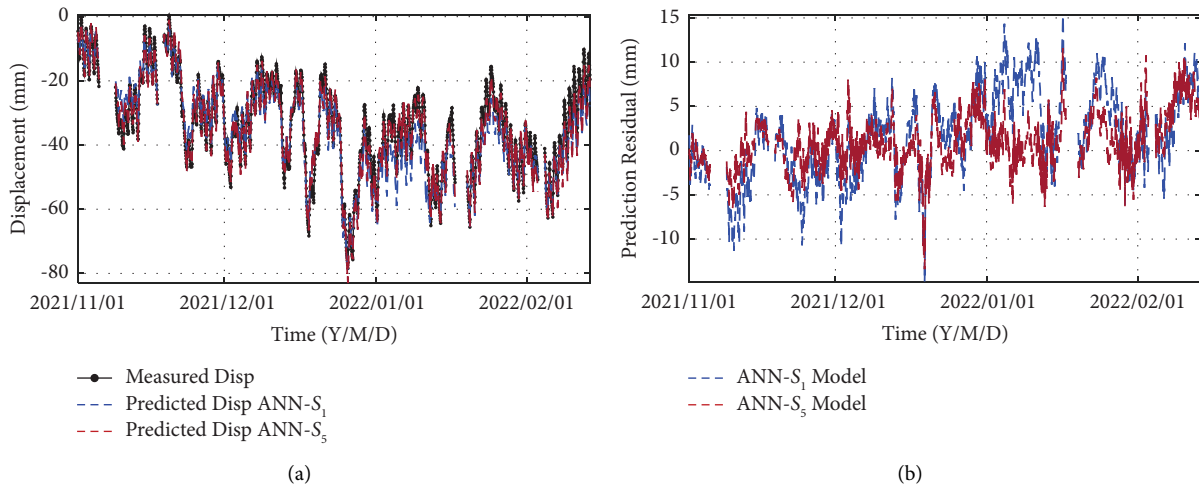

FIGURE 14: Results visualization of the optimized ANN-S_1 and ANN-S_5 models for B_3-Pier#27: (a) prediction results of the test dataset and (b) prediction residual of the test dataset.

maximum) horizontal displacement illustrated in Figures 13-14, the optimized ANN-S_5 model resulted in lower *RMSE* values for the daily extreme prediction errors of horizontal displacement compared to the optimized ANN-S_1 model, as shown in Table 5.

Based on the aforementioned discussion regarding the model performance assessment and result visualization, the optimized ANN model led to an accurate and precise horizontal displacement prediction model for a robust and reliable early warning system for bridge structures. This can be attributed to the fact that the adopted critical influencing factors efficiently model the surrounding environmental effects (D_n) by capturing the relationship between the current and previous displacements, in addition to the air temperature (T_0) with thermal inertia (T_{p-q}) and seasonal solar radiation (d) effects on the long-term horizontal displacement of bridge bearings.

5.3. Performance Comparison with Regression Models.

The prediction performance of the optimized ANN model was compared with that of multiple linear regression (MLR) and non-linear regression (MNLR) models. MLR and MNLR are the traditional statistical modeling approaches for linear and non-linear regression analyses, respectively, and are commonly used to predict the TIR, such as strain, displacement, and tilt of bridge structures [12, 21, 29–31, 40]. The MNLR model is a polynomial with a degree of measured temperature greater than one when compared to the MLR model [12, 21], and the temperature regression coefficients to predict the TIR with the MLR and MNLR models are computed based on the least-square method.

For a comparative study, the MLR and MLNR models were trained and evaluated using assessment metrics over the same training and testing periods as for the ANN model.

TABLE 5: Prediction errors of the daily extreme values of bearings' horizontal displacement with optimized ANN models.

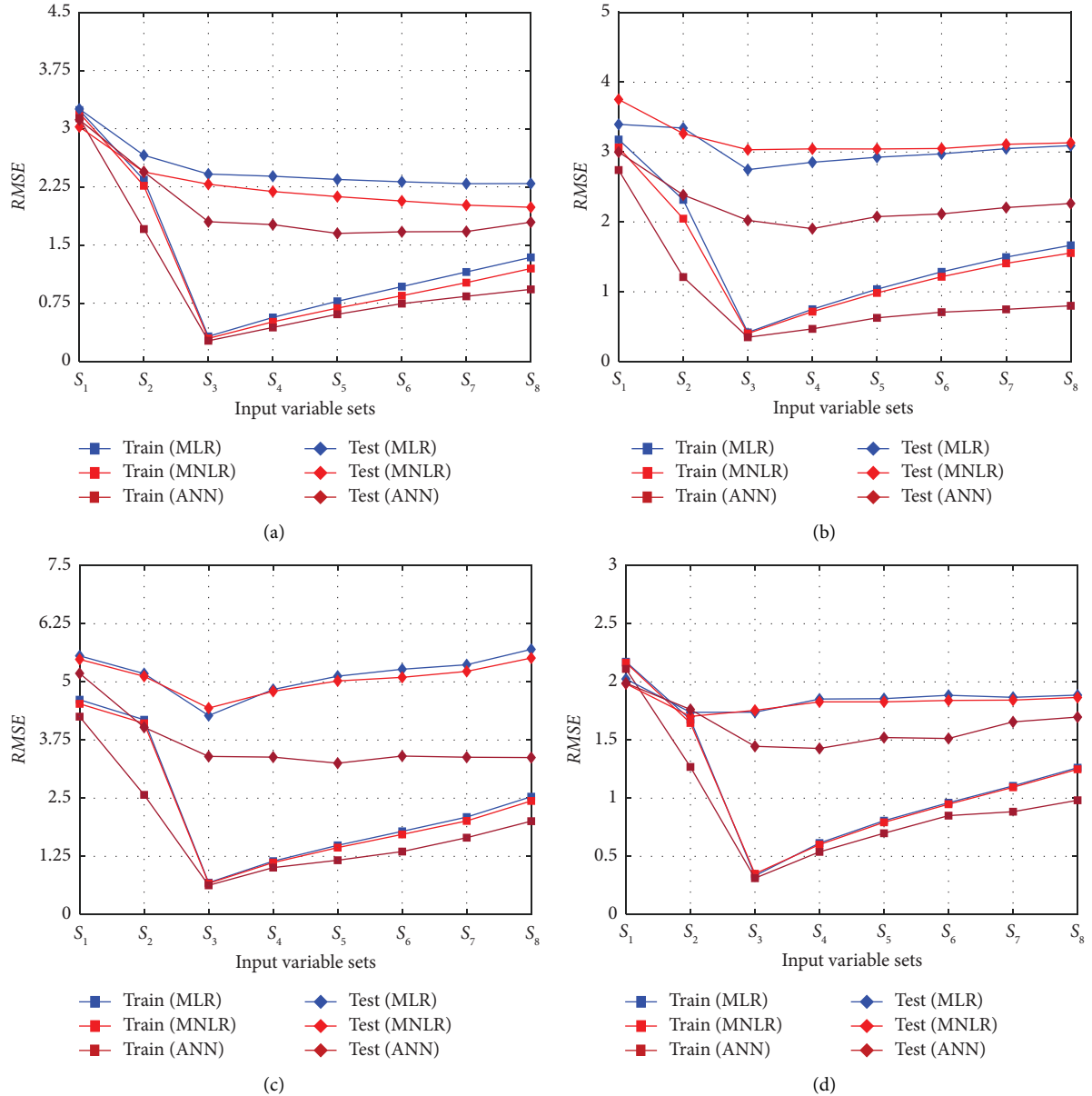| Monitored bearings	Model-influencing factors	RMSE of daily minimum displacement (mm)	RMSE of daily maximum displacement (mm)
B_1-Pier#1	ANN-S_1	3.0515	3.3792
	ANN-S_5	1.6035	1.8541
B_3-Pier#27	ANN-S_1	5.0320	5.7539
	ANN-S_5	3.2960	3.9300

FIGURE 15: Performance comparison between the MLR, MNLR, and optimized ANN models: (a) B_1-Pier#1, (b) B_2-Pier#9, (c) B_3-Pier#27, (d) B_4-Pier#34.

Figure 15 illustrates the performance comparison between the MLR, MNLR, and optimized ANN models with input variable sets S_1–S_8 for the horizontal displacement modeling of bearings B_1–B_4. Note that the temperature terms with a polynomial of degree two are adopted together with the influencing factors in the input variable sets S_1–S_8 (as listed in Table 2) to reflect the external environmental effects with the MNLR model. For instance, when the influencing factors S_3 are adopted for the MNLR model, the input variable set S_3 is modified to $\{T_0, T_0^2, T_{1\text{-}2}, T_{3\text{-}4}, T_{5\text{-}6}, T_{1\text{-}2}^2, T_{3\text{-}4}^2, T_{5\text{-}6}^2, D_1,$
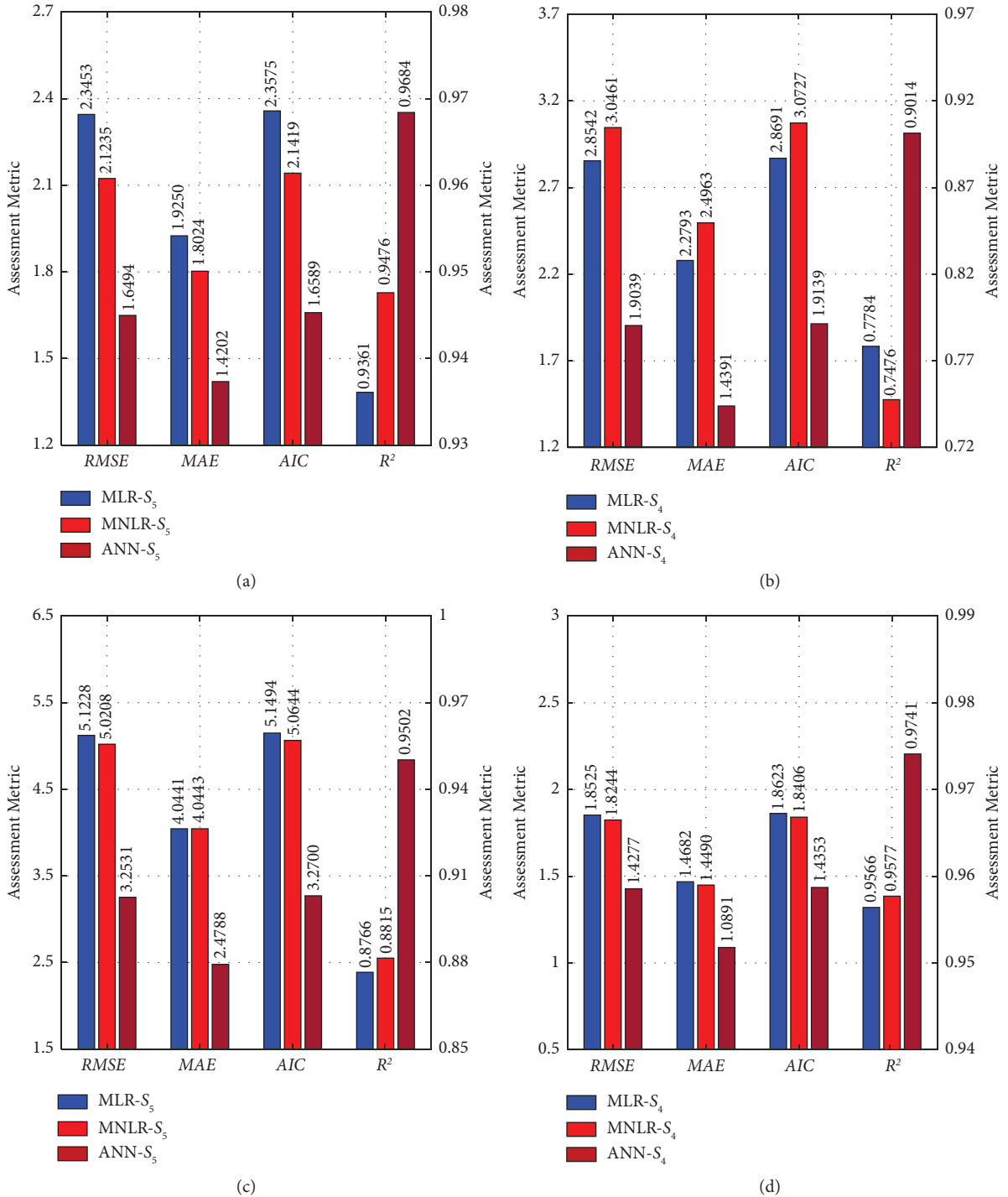
Figure 16: Direct performance assessment of the test dataset with the MLR, MNLR, and optimized ANN models employing the critical influencing factors: (a) B_1-Pier#1, (b) B_2-Pier#9, (c) B_3-Pier#27, and (d) B_4-Pier#34.

d}. In addition, when temperature terms greater than polynomial degree two are adopted, it can result in a singular modeling error as the temperature regression coefficients cannot be estimated correctly [21]. As shown in Figures 15(a)–15(d), the optimized ANN model with the proposed influencing factors adopted in the input variable sets S_3–S_8 resulted in comparatively low RMSE values

(specifically for the unseen test data). Thus, the optimized ANN model can effectively simulate the external environmental effects on the horizontal displacement of bearings B_1–B_4 compared with the MLR and MNLR models. This can be explained by the fact that the temperature regression coefficients of the MLR and MNLR models approximately fit the actual relationships between the influencing factors and
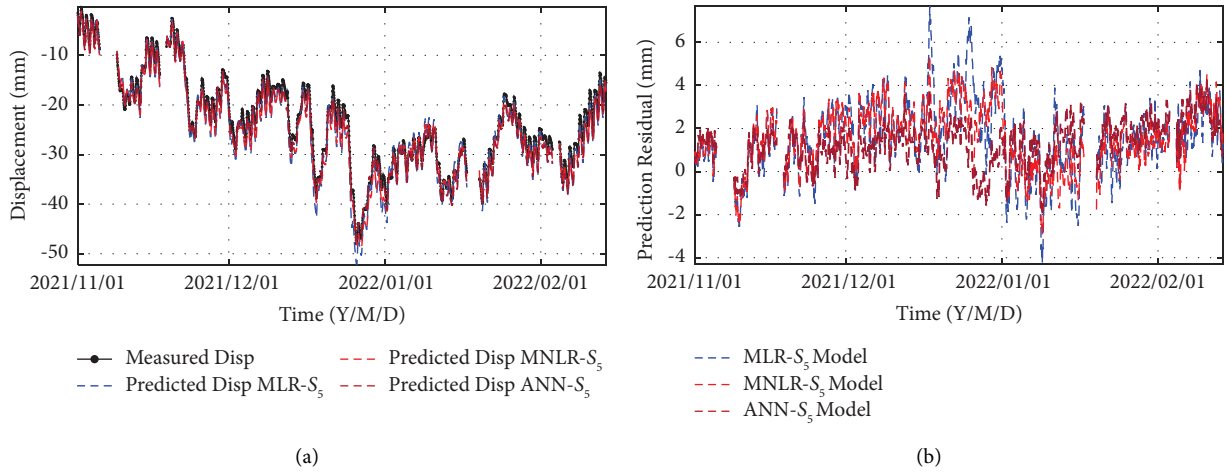
(a)   (b)

FIGURE 17: Results visualization of the MLR-S_5, MNLR-S_5, and optimally trained ANN-S_5 models for B_1-Pier#1: (a) prediction results of the test dataset and (b) prediction residual of the test dataset.

(a)   (b)

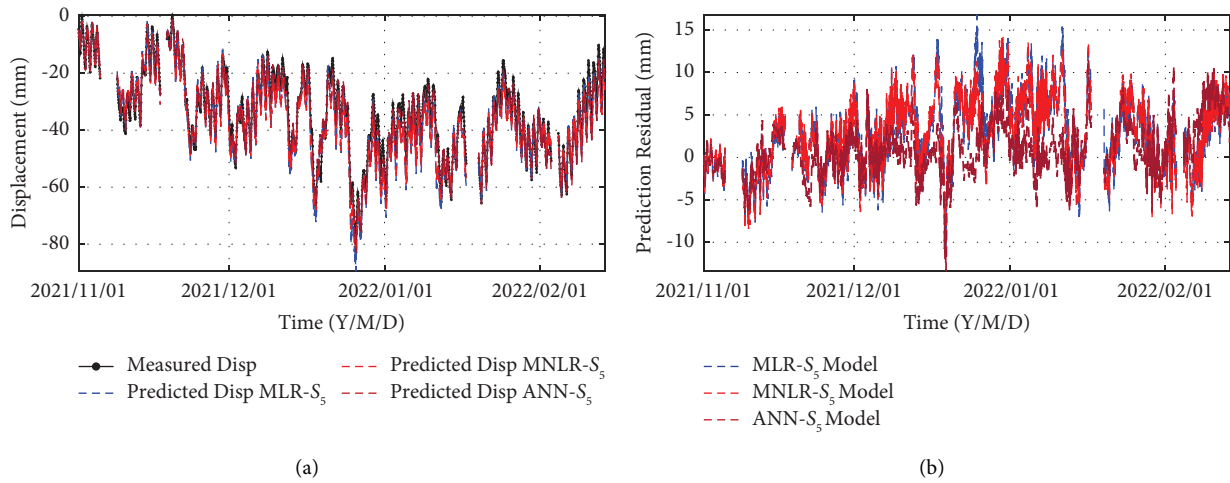FIGURE 18: Results visualization of the MLR-S_5, MNLR-S_5, and optimally trained ANN-S_5 models for B_3-Pier#27: (a) prediction results of the test dataset and (b) prediction residual of the test dataset.

TABLE 6: Prediction errors of the daily extreme values of bearings' horizontal displacement with MLR, MNLR, and optimized ANN models.

Monitored bearings	Model-influencing factors	RMSE of daily minimum displacement (mm)	RMSE of daily maximum displacement (mm)
B_1-Pier#1	MLR-S_5	2.7720	1.9205
	MNLR-S_5	2.1481	2.1447
	ANN-S_5	1.6035	1.8541
B_3-Pier#27	MLR-S_5	5.8017	5.3490
	MNLR-S_5	5.3466	5.5587
	ANN-S_5	3.2960	3.9300

TIR. Thus, it is challenging to predict the long-term horizontal displacement of bridge bearings accurately using the MLR and MNLR models.

A direct performance comparison of the test dataset in terms of the assessment metrics was also performed between the MLR, MNLR, and optimized ANN models with the critical influencing factors S_4 and S_5 for selected bearings B_1–B_4 as shown in Figures 16(a)–16(d). The optimized

ANN-S_4 and ANN-S_5 models resulted in lower prediction errors (*RMSE*, *MAE*, and *AIC*) and a better goodness of fit (R^2). For illustration purposes, the horizontal displacement prediction and amplitude of residuals by the MLR-S_5, MNLR-S_5, and optimal ANN-S_5 models for bearings B_1 and B_3 on Pier#1 and Pier#27, respectively, are plotted in Figures 17-18. Compared to those obtained with the MLR-S_5 and MNLR-S_5 models, the small amplitude fluctuation of the

optimal ANN-S_5 model illustrates a low prediction error, which resulted in a prediction that closely fits the measured horizontal displacement. To further confirm this, Table 6 illustrates the overall prediction accuracy in terms of *RMSE* of the prediction errors of daily extreme horizontal displacement of the bridge bearings shown in Figures 17-18. The optimal ANN-S_5 model resulted in lower *RMSE* values for the daily extreme prediction errors of the bearings' horizontal displacement. Hence, the optimal ANN model, in contrast to the MLR and MNLR models, efficiently modeled the linear and nonlinear relationships between the critical influencing factors and long-term horizontal displacement while dealing with high-dimensional data-mapping problems. Therefore, the optimized ANN model with the adopted critical influencing factors provides an accurate and robust prediction model to support reliable early warning systems for bridge structures.

6. Conclusion

This study proposes a modeling and prediction method for long-term horizontal displacement attributed to gradual temperature variations in a bridge structure, which is considered an essential aspect of the TBDI approach for anomaly detection in SHM. In contrast to previous studies, the proposed method employs critical influencing factors to efficiently model and predict the long-term horizontal displacement, thereby exploring the potential sources of heat exchange between the bridge structure and the external surrounding environment. A hybrid model based on an ANN with BO was utilized to determine the relationship between the critical influencing factors and long-term horizontal displacement. The viability of the presented methodology was demonstrated using long-term air temperature and bearing horizontal displacement data collected from an overpass bridge in Seoul, South Korea. The assessment metrics in terms of *RMSE*, *MAE*, *AIC*, and R^2 were used to analyze the prediction performance of the hybrid model with the critical influencing factors. The key findings of this study can be summarized as follows.

(1) The long-term horizontal displacement can be modeled accurately with the proposed comprehensive consideration of the surrounding environmental conditions by capturing the relationship between the current and past displacement information including the air temperature with thermal inertia and seasonal solar radiation effects

(2) BO is a computationally efficient method for ANN hyperparameter tuning, yielding robust optimal parameters that enhanced the ANN prediction performance for long-term horizontal displacement

(3) The optimized ANN model with the adopted critical influencing factors that effectively reflected the external environmental effects in combination resulted in a small prediction error, and generated an accurate, precise, and robust horizontal displacement prediction model

(4) Compared with the MLR and MNLR models, which are traditional statistical modeling approaches for the TIR of bridge structures, the optimized ANN model can efficiently simulate the linear and nonlinear relationships between the adopted critical influencing factors of external environmental conditions and long-term horizontal displacement, and thus exhibits the better prediction performance

In future research, the proposed method for accurate modeling and prediction of bearing long-term horizontal displacement will be investigated by integrating it with the TBDI approach for anomaly detection, which will support the implementation of a reliable early warning decision-making system for bridge structures. Furthermore, the ANN model developed with the proposed method represents a potential approach to accurately predict the bearing long-term horizontal displacement and generally can be applicable to any structural bridge and bearing types. The reason can be attributed to the capability of the developed ANN model to effectively learn and simulate the linear and complex non-linear correlations between the critical influencing factors and bearing horizontal displacement. Hence, the implementation of the proposed method will be explored on the long-term monitoring data from the other bridge structures in the future study.

Data Availability

Some or all data, models, or code generated or used during the study are proprietary or confidential in nature and may only be provided with restrictions.

Conflicts of Interest

The authors declare that they have no conflicts of interest.

Acknowledgments

References

[1] S. Moorty and C. W. Roeder, "Temperature-dependent bridge movements," *Journal of Structural Engineering*, vol. 118, no. 4, pp. 1090–1105, 1992.

[2] G.-X. Wang, Y.-L. Ding, Y.-S. Song, L.-Y. Wu, Q. Yue, and G.-H. Mao, "Detection and location of the degraded bearings based on monitoring the longitudinal expansion performance of the main girder of the Dashengguan Yangtze Bridge," *Journal of Performance of Constructed Facilities*, vol. 30, no. 4, Article ID 4015074, 2016.

[3] R. Kromanis, P. Kripakaran, and B. Harvey, "Long-term structural health monitoring of the Cleddau bridge: evaluation of quasi-static temperature effects on bearing

movements," *Structure and Infrastructure Engineering*, vol. 12, no. 10, pp. 1342–1355, 2016.

[4] B. F. Spencer, H. Jo, K. A. Mechitov et al., "Recent advances in wireless smart sensors for multi-scale monitoring and control of civil infrastructure," *Journal of Civil Structural Health Monitoring*, vol. 6, no. 1, pp. 17–41, 2016.

[5] J. M. Brownjohn, "Structural health monitoring of civil infrastructure," *Philosophical Transactions of the Royal Society A: Mathematical, Physical & Engineering Sciences*, vol. 365, no. 1851, pp. 589–622, 2007.

[6] S. Sharma, S. K. Dangi, S. K. Bairwa, and S. Sen, "Comparative study on sensitivity of acceleration and strain responses for bridge health monitoring," *Journal of Structural Integrity and Maintenance*, vol. 7, no. 4, pp. 238–251, 2022.

[7] I. A. Colombani and B. Andrawes, "A study of multi-target image-based displacement measurement approach for field testing of bridges," *Journal of Structural Integrity and Maintenance*, vol. 7, no. 4, pp. 207–216, 2022.

[8] Y. L. Xu, B. Chen, C. L. Ng, K. Y. Wong, and W. Y. Chan, "Monitoring temperature effect on a long suspension bridge," *Structural Control and Health Monitoring*, vol. 17, no. 6, pp. 632–653, 2010.

[9] N. De Battista, R. Westgate, K. Y. Koo, and J. Brownjohn, "Wireless monitoring of the longitudinal displacement of the Tamar Suspension Bridge deck under changing environmental conditions," in *Sensors and Smart Structures Technologies for Civil, Mechanical, and Aerospace Systems 2011*, International Society for Optics and Photonics, Bellingham, WA, USA, Article ID 79811O, 2011.

[10] H. Van Le and M. Nishio, "Time-series analysis of GPS monitoring data from a long-span bridge considering the global deformation due to air temperature changes," *Journal of Civil Structural Health Monitoring*, vol. 5, no. 4, pp. 415–425, 2015.

[11] H. Zhao, Y. Ding, S. Nagarajaiah, and A. Li, "Longitudinal displacement behavior and girder end reliability of a jointless steel-truss arch railway bridge during operation," *Applied Sciences*, vol. 9, no. 11, p. 2222, 2019.

[12] Y. Q. Ni, X. G. Hua, K. Y. Wong, and J. M. Ko, "Assessment of bridge expansion joints using long-term displacement and temperature measurement," *Journal of Performance of Constructed Facilities*, vol. 21, no. 2, pp. 143–151, 2007.

[13] G. T. Webb, P. J. Vardanega, P. R. A. Fidler, and C. R. Middleton, "Analysis of structural health monitoring data from Hammersmith flyover," *Journal of Bridge Engineering*, vol. 19, no. 6, Article ID 5014003, 2014.

[14] Q. Xia, Y. Cheng, J. Zhang, and F. Zhu, "In-service condition assessment of a long-span suspension bridge using temperature-induced strain data," *Journal of Bridge Engineering*, vol. 22, no. 3, Article ID 4016124, 2017.

[15] Q. Han, Q. Ma, J. Xu, and M. Liu, "Structural health monitoring research under varying temperature condition: a review," *Journal of Civil Structural Health Monitoring*, vol. 11, no. 1, pp. 149–173, 2021.

[16] D. Posenato, P. Kripakaran, D. Inaudi, and I. F. Smith, "Methodologies for model-free data interpretation of civil engineering structures," *Computers & Structures*, vol. 88, no. 7–8, pp. 467–482, 2010.

[17] D. Garcia-Sanchez, A. Fernandez-Navamuel, D. Z. Sánchez, D. Alvear, and D. Pardo, "Bearing assessment tool for longitudinal bridge performance," *Journal of Civil Structural Health Monitoring*, vol. 10, no. 5, pp. 1023–1036, 2020.

[18] F. N. Catbas, M. Susoy, and D. M. Frangopol, "Structural health monitoring and reliability estimation: long span truss bridge application with environmental monitoring data," *Engineering Structures*, vol. 30, no. 9, pp. 2347–2359, 2008.

[19] R. Kromanis and P. Kripakaran, "Support vector regression for anomaly detection from measurement histories," *Advanced Engineering Informatics*, vol. 27, no. 4, pp. 486–495, 2013.

[20] R. Kromanis and P. Kripakaran, "SHM of bridges: characterising thermal response and detecting anomaly events using a temperature-based measurement interpretation approach," *Journal of Civil Structural Health Monitoring*, vol. 6, no. 2, pp. 237–254, 2016.

[21] G.-M. Wu, T.-H. Yi, D.-H. Yang, H.-N. Li, and H. Liu, "Early warning method for bearing displacement of long-span bridges using a proposed time-varying temperature–displacement model," *Journal of Bridge Engineering*, vol. 26, no. 9, Article ID 4021068, 2021.

[22] M. T. Yarnold and F. L. Moon, "Temperature-based structural health monitoring baseline for long-span bridges," *Engineering Structures*, vol. 86, pp. 157–167, 2015.

[23] B. R. Murphy and M. T. Yarnold, "Temperature-driven assessment of a cantilever truss bridge," *Structures Congress 2017*, pp. 461–473, 2017.

[24] H. Wang, A. Li, and J. Li, "Progressive finite element model calibration of a long-span suspension bridge based on ambient vibration and static measurements," *Engineering Structures*, vol. 32, no. 9, pp. 2546–2556, 2010.

[25] R. J. Westgate and J. M. W. Brownjohn, "Development of a Tamar Bridge finite element model," in *Dynamics of Bridges*, vol. 5, pp. 13–20, Springer, Heidelberg, Germany, 2011.

[26] G.-D. Zhou and T.-H. Yi, "Thermal load in large-scale bridges: a state-of-the-art review," *International Journal of Distributed Sensor Networks*, vol. 9, no. 12, Article ID 217983, 2013.

[27] C. D. Eamon and A. S. Nowak, "Effect of secondary elements on bridge structural system reliability considering moment capacity," *Structural Safety*, vol. 26, no. 1, pp. 29–47, 2004.

[28] J.-A. Goulet, P. Kripakaran, and I. F. Smith, "Multimodel structural performance monitoring," *Journal of Structural Engineering*, vol. 136, no. 10, pp. 1309–1318, 2010.

[29] Y. Ding and A. Li, "Assessment of bridge expansion joints using long-term displacement measurement under changing environmental conditions," *Frontiers of Architecture and Civil Engineering in China*, vol. 5, no. 3, pp. 374–380, 2011.

[30] R. Kromanis and P. Kripakaran, "Predicting thermal response of bridges using regression models derived from measurement histories," *Computers & Structures*, vol. 136, pp. 64–77, 2014.

[31] Y.-L. Ding, G.-X. Wang, P. Sun, L.-Y. Wu, and Q. Yue, "Long-term structural health monitoring system for a high-speed railway bridge structure," *The Scientific World Journal*, vol. 2015, Article ID 250562, 17 pages, 2015.

[32] H. Wang, Y.-M. Zhang, J.-X. Mao, H.-P. Wan, T.-Y. Tao, and Q.-X. Zhu, "Modeling and forecasting of temperature-induced strain of a long-span bridge using an improved Bayesian dynamic linear model," *Engineering Structures*, vol. 192, pp. 220–232, 2019.

[33] H.-B. Huang, T.-H. Yi, H.-N. Li, and H. Liu, "New representative temperature for performance alarming of bridge expansion joints through temperature-displacement relationship," *Journal of Bridge Engineering*, vol. 23, no. 7, Article ID 4018043, 2018.

[34] Z.-H. Chen, X.-W. Liu, G.-D. Zhou, H. Liu, and Y.-X. Fu, "Damage detection for expansion joints of a combined highway and railway bridge based on long-term monitoring

data," *Journal of Performance of Constructed Facilities*, vol. 35, no. 4, Article ID 4021037, 2021.

[35] H.-B. Huang, T.-H. Yi, H.-N. Li, and H. Liu, "Sparse Bayesian identification of temperature-displacement model for performance assessment and early warning of bridge bearings," *Journal of Structural Engineering*, vol. 148, no. 6, Article ID 4022052, 2022.

[36] G.-D. Zhou, T.-H. Yi, B. Chen, and X. Chen, "Modeling deformation induced by thermal loading using long-term bridge monitoring data," *Journal of Performance of Constructed Facilities*, vol. 32, no. 3, Article ID 4018011, 2018.

[37] H. Abdel-Jaber and B. Glisic, "Systematic method for the validation of long-term temperature measurements," *Smart Materials and Structures*, vol. 25, no. 12, Article ID 125025, 2016.

[38] B. K. Oh, H. S. Park, and B. Glisic, "Prediction of long-term strain in concrete structure using convolutional neural networks, air temperature and time stamp of measurements," *Automation in Construction*, vol. 126, Article ID 103665, 2021.

[39] D. Zhao, Y. Ren, Q. Huang, and X. Xu, "Analysis of temperature-induced deflection of cable-stayed bridge based on BP neural network," in *IOP Conference Series: Earth and Environmental Science*, IOP Publishing, Bristol, UK, Article ID 62075, 2019.

[40] Q. Huang, M. Crosetto, O. Monserrat, and B. Crippa, "Displacement monitoring and modelling of a high-speed railway bridge using C-band Sentinel-1 data," *ISPRS Journal of Photogrammetry and Remote Sensing*, vol. 128, pp. 204–211, 2017.

[41] L. Zhou, L. Chen, Y. Xia, and K. Y. Koo, "Temperature-induced structural static responses of a long-span steel box girder suspension bridge," *Journal of Zhejiang University - Science*, vol. 21, no. 7, pp. 580–592, 2020.

[42] S.-H. Kim, S.-J. Park, J. Wu, and J.-H. Won, "Temperature variation in steel box girders of cable-stayed bridges during construction," *Journal of Constructional Steel Research*, vol. 112, pp. 80–92, 2015.

[43] H. F. Zhou, Y. Q. Ni, and J. M. Ko, "Constructing input to neural networks for modeling temperature-caused modal variability: mean temperatures, effective temperatures, and principal components of temperatures," *Engineering Structures*, vol. 32, no. 6, pp. 1747–1759, 2010.

[44] J. Mata, "Interpretation of concrete dam behaviour with artificial neural network and multiple linear regression models," *Engineering Structures*, vol. 33, no. 3, pp. 903–910, 2011.

[45] B. K. Oh, B. Glisic, S. W. Park, and H. S. Park, "Neural network-based seismic response prediction model for building structures using artificial earthquakes," *Journal of Sound and Vibration*, vol. 468, Article ID 115109, 2020.

[46] F. J. Diez, L. M. Navas-Gracia, L. Chico-Santamarta, A. Correa-Guimaraes, and A. Martínez-Rodríguez, "Prediction of horizontal daily global solar irradiation using artificial neural networks (ANNs) in the castile and león region, Spain," *Agronomy*, vol. 10, no. 1, p. 96, 2020.

[47] T.-T. Le, "Surrogate neural network model for prediction of load-bearing capacity of CFSS members considering loading eccentricity," *Applied Sciences*, vol. 10, no. 10, p. 3452, 2020.

[48] H. S. Moon, S. Ok, P. Chun, and Y. M. Lim, "Artificial neural network for vertical displacement prediction of a bridge from strains (Part 1): girder bridge under moving vehicles," *Applied Sciences*, vol. 9, no. 14, p. 2881, 2019.

[49] X. Han, H. Xiang, Y. Li, and Y. Wang, "Predictions of vertical train-bridge response using artificial neural network-based surrogate model," *Advances in Structural Engineering*, vol. 22, no. 12, pp. 2712–2723, 2019.

[50] A. Ruffels, I. Gonzalez, and R. Karoumi, "Model-free damage detection of a laboratory bridge using artificial neural networks," *Journal of Civil Structural Health Monitoring*, vol. 10, no. 2, pp. 183–195, 2020.

[51] H. Li, T. Wang, and G. Wu, "Dynamic response prediction of vehicle-bridge interaction system using feedforward neural network and deep long short-term memory network," in *Structures*, pp. 2415–2431, Elsevier, 2021.

[52] H. S. Moon, Y. K. Hwang, M. K. Kim, H.-T. Kang, and Y. M. Lim, "Application of artificial neural network to predict dynamic displacements from measured strains for a highway bridge under traffic loads," *Journal of Civil Structural Health Monitoring*, vol. 12, pp. 117–126, 2022.

[53] B. Stojanovic, M. Milivojevic, N. Milivojevic, and D. Antonijevic, "A self-tuning system for dam behavior modeling based on evolving artificial neural networks," *Advances in Engineering Software*, vol. 97, pp. 85–95, 2016.

[54] P. G. Benardos and G.-C. Vosniakos, "Optimizing feedforward artificial neural network architecture," *Engineering Applications of Artificial Intelligence*, vol. 20, no. 3, pp. 365–382, 2007.

[55] G. Zhang, B. Eddy Patuwo, and M. Y Hu, *International Journal of Forecasting*, vol. 14, no. 1, pp. 35–62, 1998.

[56] B. Shahriari, K. Swersky, Z. Wang, R. P. Adams, and N. De Freitas, "Taking the human out of the loop: a review of Bayesian optimization," *Proceedings of the IEEE*, vol. 104, no. 1, pp. 148–175, 2016.

[57] J. Wu, X.-Y. Chen, H. Zhang, L.-D. Xiong, H. Lei, and S.-H. Deng, "Hyperparameter optimization for machine learning models based on Bayesian optimization," *J. Electron. Sci. Technol*, vol. 17, no. 1, pp. 26–40, 2019.

[58] M. I. Sameen, B. Pradhan, and S. Lee, "Application of convolutional neural networks featuring Bayesian optimization for landslide susceptibility assessment," *Catena*, vol. 186, Article ID 104249, 2020.

[59] Y.-M. Zhang, H. Wang, J.-X. Mao, Z.-D. Xu, and Y.-F. Zhang, "Probabilistic framework with bayesian optimization for predicting typhoon-induced dynamic responses of a long-span bridge," *Journal of Structural Engineering*, vol. 147, no. 1, Article ID 4020297, 2021.

[60] W. S. McCulloch and W. Pitts, "A logical calculus of the ideas immanent in nervous activity," *Bulletin of Mathematical Biophysics*, vol. 5, no. 4, pp. 115–133, 1943.

[61] F. Kang, J. Liu, J. Li, and S. Li, "Concrete dam deformation prediction model for health monitoring based on extreme learning machine," *Structural Control and Health Monitoring*, vol. 24, no. 10, p. 1997, 2017.

[62] F. Kang, J. Li, S. Zhao, and Y. Wang, "Structural health monitoring of concrete dams using long-term air temperature for thermal effect simulation," *Engineering Structures*, vol. 180, pp. 642–653, 2019.

[63] F. Kang and J. Li, "Displacement model for concrete dam safety monitoring via Gaussian process regression considering extreme air temperature," *Journal of Structural Engineering*, vol. 146, no. 1, Article ID 5019001, 2020.

[64] K. Naidu, M. S. Ali, A. H. Abu Bakar, C. K. Tan, H. Arof, and H. Mokhlis, "Optimized artificial neural network to improve the accuracy of estimated fault impedances and distances for underground distribution system," *PLoS One*, vol. 15, no. 1, Article ID 227494, 2020.

[65] MATLAB, "Neural network toolbox user's guide," p. 846, 2004, http://cda.psych.uiuc.edu/matlab_pdf/nnet.pdf.

[66] B. Kim, J. Lee, S.-H. Sim, S. Cho, and B. H. Park, "Computer vision-based remote displacement monitoring system for insitu bridge bearings robust to large displacement induced by temperature change," *Smart Structures and Systems*, vol. 30, no. 5, pp. 521–535, 2022.

[67] E. Brochu, V. M. Cora, and N. De Freitas, "A tutorial on Bayesian optimization of expensive cost functions, with application to active user modeling and hierarchical reinforcement learning," 2010, https://arxiv.org/abs/1012.2599.

[68] J. Bergstra and Y. Bengio, "Random search for hyperparameter optimization," *Journal of Machine Learning Research*, vol. 13, no. 2, 2012.